

ETH-Tight Complexity of Optimal Morse Matching on Bounded-Treewidth Complexes

Geevarghese Philip  

Chennai Mathematical Institute, Chennai, India, and IRL ReLaX

Erlend Raa Vågset  

Western Norway University of Applied Sciences (HVL), Førde, Norway

Abstract

The OPTIMAL MORSE MATCHING (OMM) problem asks for a discrete gradient vector field on a simplicial complex that minimizes the number of critical simplices. It is NP-hard and has been studied extensively in heuristic, approximation, and parameterized complexity settings. Parameterized by treewidth k , OMM has long been known to be solvable on triangulations of 3-manifolds in $2^{O(k^2)}n^{O(1)}$ time and in FPT time for triangulations of arbitrary manifolds, but the exact dependence on k has remained an open question. We resolve this by giving a new $2^{O(k \log k)}n$ -time algorithm for any finite regular CW complex, and show that no $2^{o(k \log k)}n^{O(1)}$ -time algorithm exists unless the Exponential Time Hypothesis (ETH) fails.

2012 ACM Subject Classification Theory of computation \rightarrow Parameterized complexity and exact algorithms; Theory of computation \rightarrow Algorithm design techniques; Mathematics of computing \rightarrow Combinatorial algorithms; Applied computing \rightarrow Computational topology

Keywords and phrases Discrete Morse Theory, Simplicial Complexes, Optimal Morse Matching, Treewidth, Parameterized Algorithms, Computational Topology, Dynamic Programming, Exponential Time Hypothesis, Topological Data Analysis.

Funding *Erlend Raa Vågset*: Supported in part by the Research Council of Norway, grant “Parameterized Complexity for Practical Computing (PCPC)” (No. 274526).

1 Introduction

Classical Morse theory [37] and its discrete counterpart [21, 22] provide a framework for simplifying spaces while preserving their essential topological features (see Figure 1). They do so by relating scalar functions to gradient flows in the smooth setting and discrete Morse functions to discrete gradient vector fields (Morse matchings) in the combinatorial setting. Much of the computational work on discrete Morse theory has focused on the matching perspective [32, 34, 39, 27, 1, 23], with the pioneering work on treewidth in computational topology [12] being no exception. At first sight, this close relationship suggests that the two formulations are interchangeable. In reality, they form diverging roads in the algorithmic landscape; let us follow the one less traveled by.

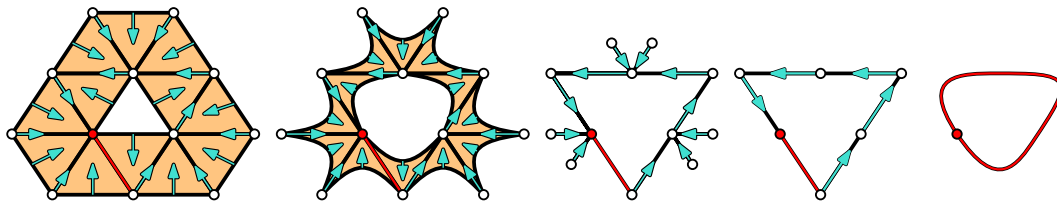


Figure 1 Discrete Morse theory can simplify a space while preserving its homotopy type.

Morse theory has applications in topological data analysis and computational topology [27, 2, 33, 38, 23, 16], robotics and configuration spaces [20, 24], molecular modeling [14], and

mesh and image processing [35, 18]. A recurring primitive in these works is to construct a discrete gradient vector field, also known as a Morse matching, with few critical simplices, yielding strong homotopy-preserving simplifications. Intuitively, such a field is a discrete vector field without “swirls”: there are no loops in the flow lines, so one can contract the space along them without changing the homotopy type. Combinatorially, such a field corresponds to a matching in the Hasse diagram of the complex such that reversing the matched edges does not create any directed cycles. This motivates the OPTIMAL MORSE MATCHING (OMM) problem, also known as MIN-/MAX-MORSE MATCHING, depending on whether the objective is to minimize the number of critical simplices or maximize the number of matched pairs:

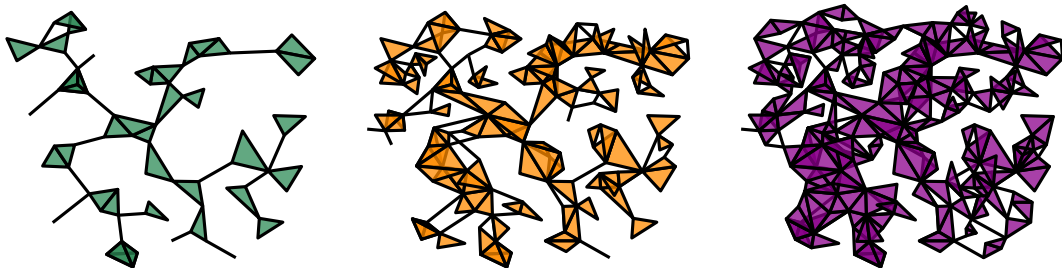
Problem 1. Optimal Morse Matching (OMM)

Input: A finite simplicial complex K and a weight function $\omega : K \rightarrow \mathbb{R}_{\geq 0}$.

Task: Find a discrete gradient vector field W on K .

Optimize: Minimize the total weight of critical (i.e., unmatched) simplices.

From a computational complexity perspective, OMM and closely related variants are highly intractable: they are NP-hard [32], admit strong classical inapproximability bounds [3], and are linked to other hard topological decision problems such as COLLAPSIBILITY [41, 36], ERASIBILITY of 2-complexes [12, 3], and SHELLABILITY [25]. Algorithmic work includes approximation algorithms for MAX-MORSE MATCHING [39] and a variety of heuristic and workflow-based methods for practical simplification [2, 34, 27, 23, 1]. On the parameterized side, using the optimum number of critical simplices as parameter, ERASIBILITY and MIN-MORSE MATCHING are W[P]-hard and admit no FPT approximation schemes [12, 4].



■ **Figure 2** Three spaces from left to right, all of relatively low (but increasing) treewidth.

To circumvent these complexity barriers we turn to treewidth, which intuitively measures how close a combinatorial object is to being a tree; see Figure 2. An early systematic use of treewidth in discrete Morse theory is the fixed-parameter algorithm of [12] for OMM, which runs in time $2^{O(t^2)}n^{O(1)}$ when parameterized by the treewidth t of an associated spine graph for 2-complexes, and by the treewidth of either the spine graph or the dual graph for triangulated 3-manifolds. This was complemented by a Courcelle-style metatheorem for MSO-definable properties on triangulations [11], which yields fixed-parameter tractability for OMM on triangulated manifolds of fixed dimension when parameterized by the treewidth of the dual graph. Since then, treewidth has become central in computational topology, leading to FPT algorithms for a range of NP-hard topological problems and invariants [10, 13, 6], ETH-tight lower bounds for several of these problems [8, 5, 7, 42], and detailed studies of the width of triangulated 3-manifolds [30, 28, 29].

► **Remark 2.** Across the literature, “treewidth k ” is measured on different associated graphs (dual graphs, spine graphs, Hasse diagrams), chosen to suit the problem at hand. For fixed

dimension, [11] shows that the treewidth of the Hasse diagram of a triangulation is bounded by a constant factor times the treewidth of its dual graph, and [12] shows that in dimension 3 the spine treewidth is likewise linearly bounded in terms of the dual treewidth. Thus, for fixed dimension these parameters coincide up to constant factors hidden in the $O(\cdot)$ -notation. In this paper we simply write “treewidth k ” and, in practice, work with the Hasse diagram.

1.1 Contributions

Algorithmic. We give an explicit dynamic program (DP) for a digraph formulation of OPTIMAL MORSE MATCHING parameterized by treewidth k , which in particular solves OMM on all finite regular CW complexes of treewidth k . It runs in time $2^{O(k \log k)}n$, thereby extending and improving both the earlier explicit treewidth-based algorithms for 2-complexes and triangulated 3-manifolds with running time $2^{O(k^2)}n^{O(1)}$ [12] and the implicit MSO-based algorithm for triangulated manifolds in [11]. The simple invariant and state space allowed us to implement the algorithm and verify it on small instances by exhaustive search.

Optimality. Under ETH, our running time is optimal: using a known treewidth-based lower bound for DIRECTED FEEDBACK VERTEX SET (DFVS), we show that there is no $2^{o(k \log k)}n^{O(1)}$ -time algorithm for OPTIMAL MORSE MATCHING parameterized by treewidth k , even on 2-dimensional complexes of top coface degree at most 4. This follows from a new polynomial-time reduction from DFVS to ERASABILITY, to which we apply the recent Width Preserving Strategy (WiPS) framework of [42] to ensure that treewidth is preserved. Combined with the standard equivalence between ERASABILITY and OMM on 2-dimensional complexes, this yields the ETH-tight $2^{\Theta(k \log k)}$ dependence.

Conceptual: Our order-based formulation (FEEDBACK MORSE ORDER) shows that working indirectly with vertex orders rather than directly with matchings captures exactly what a treewidth DP for OMM needs to remember. This ordering viewpoint transfers to ALTERNATING CYCLE-FREE/UNIQUELY RESTRICTED MATCHINGS (AC-FM/URM) on bipartite graphs, but the connection breaks on general graphs. Here, AC-FM and URM still only admit $2^{\Theta(k^2)}n^{O(1)}$ -time algorithms and lack tight-ETH lower bounds. We therefore point to AC-FM and URM as natural candidates for genuinely $2^{\Theta(k^2)}$ -time problems in treewidth and as targets for either $2^{O(k \log k)}n$ -time algorithms or matching $2^{o(k^2)}n^{O(1)}$ lower bounds.

► **Remark 3.** This document is the full version of our paper accepted for presentation at the ACM Symposium on Computational Geometry (SoCG 2026). It includes full proofs and additional technical details provided in the appendices.

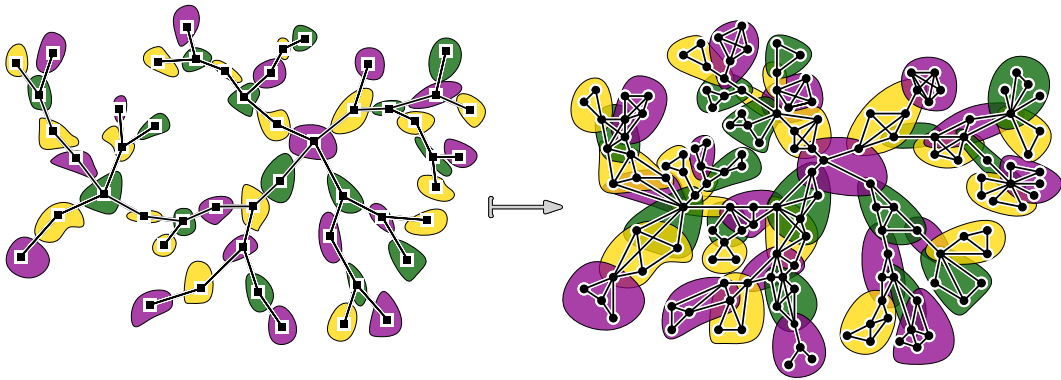
2 Preliminaries

We use standard terminology from parameterized complexity [19, 17] and discrete Morse theory [21, 22, 40]. We write n for the input size; for OMM, n is the number of cells of the complex, which equals the number of vertices of its Hasse diagram.

2.1 Parameterized complexity theory

Treewidth and nice tree decompositions. When we speak of the treewidth of a digraph or a complex, we mean the treewidth of the natural underlying undirected graph in the first case, and of the Hasse diagram in the second. Informally, treewidth measures how close a graph is to being a tree (see also Figure 2): we cover the graph by overlapping bags of vertices arranged in a tree so that each edge lies entirely inside some bag and the bags containing any fixed vertex form a connected subtree; the width is one less than the size of

the largest bag, and the treewidth k is the minimum width over all such decompositions; this k will be our parameter throughout the paper. Such decompositions let us localize global constraints: a dynamic program only needs to maintain partial solutions on a bag of size $k + 1$ and combine them along the tree, so we can brute-force over states per bag rather than over the whole graph and obtain running times of the form $f(k) n^{O(1)}$. We use rooted nice tree decompositions; unless stated otherwise, we fix an arbitrary root bag and process the decomposition bottom-up. Formal definitions are given in Appendix A.1. In this paper we work with the standard nice node types (leaf, introduce-vertex, forget-vertex, and join), and we also use auxiliary *introduce-edge* bags: unary nodes whose bag is identical to that of their child and that are annotated with a single edge uv in the bag, marking the point where that edge is processed in the dynamic program or reduction. This is a standard refinement that preserves width.



■ **Figure 3** A graph G (right) and a tree decomposition T (left). Each node of T carries a bag $X_t \subseteq V(G)$, drawn as a blob containing vertices of G . Adjacent bags overlap so that every vertex and every edge of G is covered.

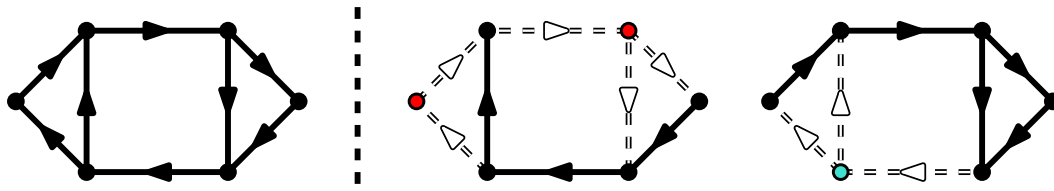
FPT and ETH. A parameterized problem with parameter k is *fixed-parameter tractable* (FPT) if it can be solved in time $f(k) n^{O(1)}$ for some computable function f ; such running times are considered efficient when k is small compared to n , since the combinatorial explosion is confined to $f(k)$ while the dependence on the input size remains polynomial. For conditional lower bounds we assume the *Exponential Time Hypothesis* (ETH) [31], which states that 3-SAT on n variables cannot be solved in time $2^{o(n)}$; ETH is a strengthening of $P \neq NP$ that has withstood decades of algorithmic progress and underpins many tight running-time lower bounds. Our hardness source is DIRECTED FEEDBACK VERTEX SET parameterized by the treewidth k of the underlying undirected graph of the input digraph D , where a *feedback vertex set* in a digraph $D = (V, E)$ is a set $J \subseteq V$ such that $D \setminus J$ is acyclic.

Problem 4. Directed Feedback Vertex Set (DFVS)

Input: A directed graph $D = (V, E)$ and an integer s .

Question: Does D contain a feedback vertex set of size at most s ?

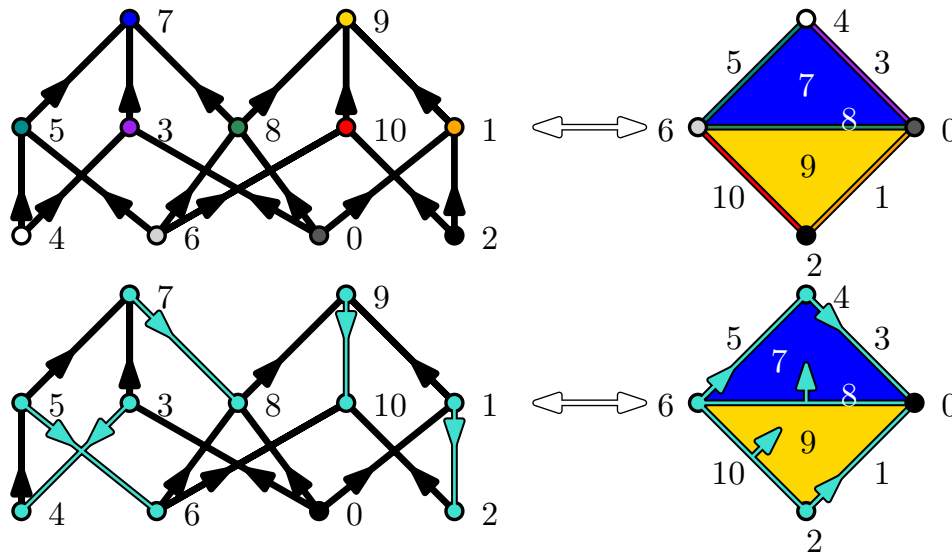
► **Theorem 5** (Bonamy et al. [9]). *Unless ETH fails, DFVS parameterized by the treewidth k of the underlying undirected graph of the input digraph cannot be solved in $2^{o(k \log k)} n^{O(1)}$ -time.*



■ **Figure 4** An instance of DFVS, a valid solution of size 2 and an optimal solution of size 1.

2.2 Discrete Morse theory

Complexes and Hasse diagrams. See Forman [21] for formal definitions of finite regular CW complexes and discrete Morse theory; we keep preliminaries brief since our algorithms are graph-theoretic and the lower bound holds already for simplicial complexes. Face relations are given by closure containment, so the face poset and its directed Hasse diagram encode the incidence data we use. We write $\vec{H}(X)$ for the directed Hasse diagram of a complex X ; it has one vertex per cell and an arc $\sigma \rightarrow \tau$ whenever σ is an immediate face of τ (a cover relation in the face poset), and hence $\dim(\tau) = \dim(\sigma) + 1$. Let $H(X)$ be the underlying undirected graph; we measure treewidth on $H(X)$, denoted k . Simplicial complexes are the special case where cells are simplices (points, lines, triangles, tetrahedra, etc.); we use them in figures and in our reduction.

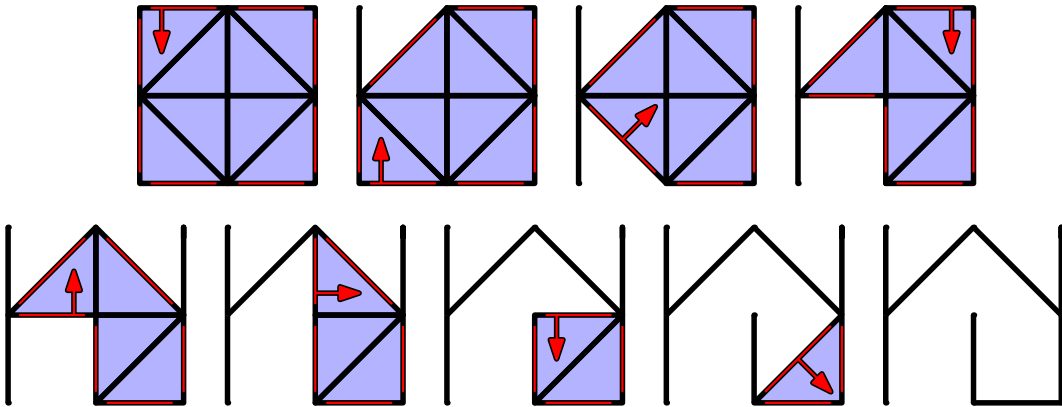


■ **Figure 5** A discrete Morse function (top) on the Hasse diagram of a simplicial complex (left) and its geometric realization (right). Below, the induced discrete gradient vector field (Morse matching) is shown both on the Hasse diagram (left) and geometrically as a gradient vector field (right).

Discrete Morse theory on complexes. Forman’s discrete Morse theory can be phrased entirely in terms of matchings on the Hasse diagram $\vec{H}(X)$ of a finite regular CW complex X . A *discrete vector field* is a matching W on $\vec{H}(X)$, i.e. a set of pairs (σ, τ) with $\sigma \rightarrow \tau$ an arc of $\vec{H}(X)$ such that each cell appears in at most one pair. From W we obtain a new digraph $\vec{H}(X)_W$ by reversing exactly the matched arcs and leaving all others unchanged; if $\vec{H}(X)_W$ is acyclic, then W is a *discrete gradient vector field*. Forman’s correspondence states that (i) every discrete Morse function on X induces such a gradient vector field, and (ii)

conversely, every discrete gradient vector field arises from some discrete Morse function; in both directions, the unmatched cells in W are precisely the critical cells of the corresponding Morse function. Collapsing X along the gradient flow yields a smaller Morse complex (see Figure 1) that is homotopy equivalent to X and can make downstream topological computations much cheaper. The OPTIMAL MORSE MATCHING problem (Problem 1) asks for a discrete gradient vector field minimizing the total weight of these unmatched cells.

Erasibility in 2D. For our lower bound we use the notion of *erasibility* of 2-dimensional simplicial complexes K . A 1-simplex (edge) e is *free* if it is contained in exactly one 2-simplex τ , and removing e together with τ is an *elementary collapse*. A 2-simplex is *erasible* if it can be removed through a sequence of elementary collapses, and K is *erasible* if every 2-simplex can be eliminated in this way, that is, if K collapses to a 1-dimensional complex.



■ **Figure 6** A triangulation of a square that is erasible with $S = \emptyset$: free edges are marked in red and elementary collapses by arrows. In contrast, a triangulation of a sphere has no free edges, so any erasibility requires $|S| > 0$.

Problem 6. Erasibility

Input: A 2-dimensional simplicial complex K and an integer $B \geq 0$.

Question: Is there a set S of 2-simplices in K such that $|S| \leq B$ and $K \setminus S$ is erasible?

► **Theorem 7** (Folklore; cf. [21, 32, 3]). *For finite 2-dimensional simplicial complexes, ERASIBILITY and OPTIMAL MORSE MATCHING are computationally equivalent.*

3 Algorithm

We give a fixed-parameter algorithm for FEEDBACK MORSE MATCHING, a digraph generalization of OPTIMAL MORSE MATCHING, on digraphs whose underlying undirected graph has treewidth k . The algorithm rests on three ingredients: (i) we work in the general setting of arbitrary digraphs rather than Hasse diagrams only; (ii) we adopt the Morse-function viewpoint and encode solutions as vertex orders (FEEDBACK MORSE ORDERS) instead of matchings; and (iii) this yields a very simple dynamic program whose state at each bag consists only of an order on the bag and a subset of its vertices. This order-mask formulation avoids the more involved connectivity machinery of previous approaches and leads to a running time of $2^{O(k \log k)} n$.

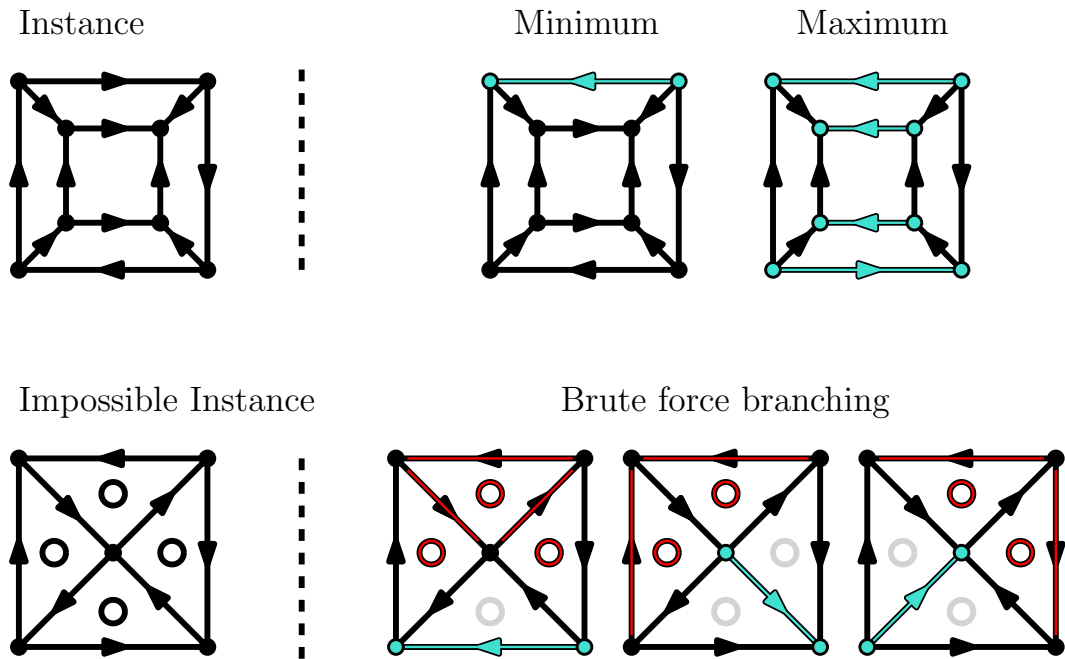
3.1 Of feedback Morse matchings and feedback Morse orders

Generalizing OMM to digraphs. For our algorithmic purposes it is convenient to generalize the matching viewpoint from Hasse diagrams to arbitrary digraphs, and to allow both positive and negative weights. Given a digraph $D = (V, E)$ and a matching $M \subseteq E$, let D_M be the digraph obtained by reversing every edge of M and leaving all other edges unchanged; we call M a *feedback Morse matching* if D_M is acyclic. In the resulting FEEDBACK MORSE MATCHING (FMM) problem (Problem 8), the input is a digraph D and a weight function $\omega : V(D) \rightarrow \mathbb{R}$, and the task is to find a feedback Morse matching minimizing the total weight of unmatched vertices. When D is the Hasse diagram $\vec{H}(K)$ of a simplicial complex K and $V(D)$ is identified with the simplices of K , discrete gradient vector fields on K are exactly feedback Morse matchings on D . Thus OMM is the special case of FMM where D comes from a complex and ω is nonnegative; in the classical unweighted case $\omega \equiv 1$, the objective is simply the number of critical simplices [32, 3]. Mixed-sign weights in this framework allow one to favour or penalize particular cells (useful for extending a Morse Matching), while the purely negative-weight variant (e.g. $\omega \equiv -1$) on general digraphs corresponds to finding a smallest feedback Morse matching, that is, a minimum-size matching whose reversals destroy all directed cycles in D .

Problem 8. Feedback Morse Matching (FMM)

Input: A finite directed graph $D = (V, E)$ and a weight function $\omega : V(D) \rightarrow \mathbb{R}$.

Question: Find a feedback Morse matching $M \subseteq E(D)$ that minimizes the total weight of unmatched vertices.



■ **Figure 7** Feedback Morse matchings on digraphs. Top: an instance that admits feedback Morse matchings; two optimal solutions to FMM are shown. Bottom: an instance with no feedback Morse matching.

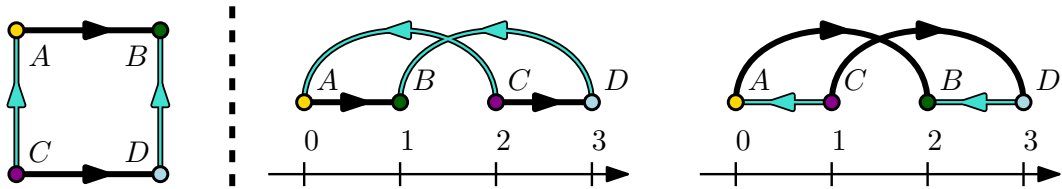
► **Theorem 9.** Let $D = (V, E)$ be a digraph whose underlying undirected graph has treewidth k , and let $n := |V(D)|$. Given vertex weights $\omega : V \rightarrow \mathbb{R}$, FEEDBACK MORSE MATCHING on (D, ω) can be solved in time $2^{O(k \log k)} n$.

Shifting from matchings to orders. As committed procrastinators, we now do our best to avoid thinking about matchings. Instead, we turn to vertex orders. Let $\pi = (v_1, \dots, v_n)$ be a total order of V . An edge $(u, v) \in E$ is *backward* with respect to π if v appears before u in π , and let $M(\pi) := \{(u, v) \in E : (u, v) \text{ is backward w.r.t. } \pi\}$ be the set of backward edges. Once π is fixed, the set of edges to reverse is determined: we always take $M(\pi)$ and reverse exactly these edges. We call π a *feedback Morse order* if $M(\pi)$ is a matching (no two edges in $M(\pi)$ share a vertex).

Problem 10. Feedback Morse Order (FMO)

Input: A digraph $D = (V, E)$ and a weight function $\omega : V \rightarrow \mathbb{R}$.

Question: Find a feedback Morse order π that minimizes the total weight of vertices that are unmatched in $M(\pi)$.



■ **Figure 8** Two feedback Morse orders of the same digraph, drawn as permutations of the vertices. In both orders, the same set of backward edges (highlighted) forms a feedback Morse matching M , showing that one matching may admit many compatible orders; other orders can yield different backward-edge sets (and different matchings), or even no matching at all. For example, $D \prec C \prec B \prec A$ induces the other optimal matching $\{A \rightarrow B, C \rightarrow D\}$, $C \prec D \prec B \prec A$ induces only $\{A \rightarrow B\}$, and $A \prec D \prec C \prec B$ has backward edges $C \rightarrow A$ and $D \rightarrow C$, which is not a matching.

► **Lemma 11 (Matchings vs. orders).** Let $D = (V, E)$ be a digraph. If π is a feedback Morse order, then $M(\pi)$ is a feedback Morse matching on D . Conversely, if M is a feedback Morse matching on D , then there exists a feedback Morse order π with $M(\pi) = M$.

Proof. For any order π , reversing all backward edges makes every edge point forward along π , so reversing all backward edges yields an acyclic digraph; if $M(\pi)$ is a matching, it is a feedback Morse matching. Conversely, if M is a feedback Morse matching, then D_M is acyclic, and any topological order π of D_M satisfies $M(\pi) = M$. ◀

A Forman correspondence. By Lemma 11, FMO and FMM are equivalent optimization problems: every optimal feedback Morse order induces an optimal feedback Morse matching and vice versa, so in what follows we work entirely with the order-based formulation.

3.2 R-FMO: The boundary subproblem on bags

Orders and masks on bags. We run our dynamic program over a rooted nice tree decomposition of the underlying undirected graph of D , refined with introduce-edge bags as in Section 2. For a bag t let X_t be its vertex set, T_t the subtree rooted at t , W_t the vertices

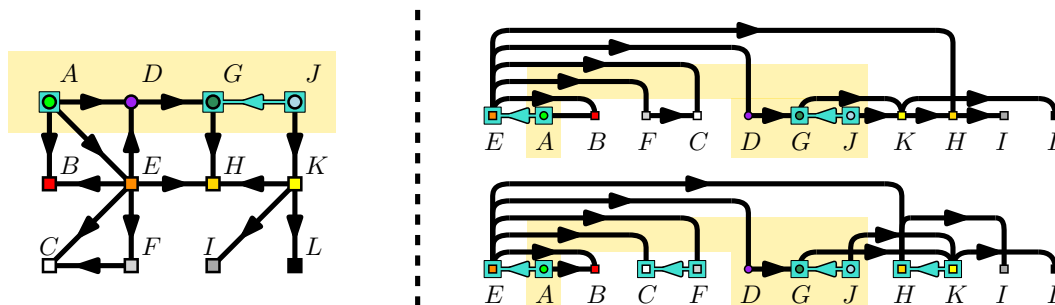
appearing in bags of T_t , and G_t the subgraph on W_t whose edges are exactly those whose introduce-edge bags lie in T_t . Intuitively, G_t is the part of the graph already processed when we are at t , and X_t is its boundary. A global feedback Morse order π on D restricts at t to a total order g on X_t and a set $U \subseteq X_t$ of boundary vertices already matched inside G_t ; we view U as a mask on X_t , marking which boundary vertices are already matched. This leads to the following boundary subproblem.

Problem 12. Restricted Feedback Morse Order (R-FMO)

Input: A digraph $G = (W, E')$ with vertex weights $\omega : W \rightarrow \mathbb{R}$, a boundary set $X \subseteq W$, a total order g of X , and a subset $U \subseteq X$.

Question: Among all feedback Morse orders π on G with $\pi|_X = g$ and $V(M(\pi)) \cap X = U$, minimize $\sum_{v \in W \setminus X : v \notin V(M(\pi))} \omega(v)$; if no such π exists, the optimum is defined as $+\infty$.

The global optimum of FMO (and hence of FMM) is the value of an R-FMO instance at the root bag, whose boundary is empty; in particular, every state in our dynamic program will consist of an order on the bag together with a mask of matched boundary vertices.



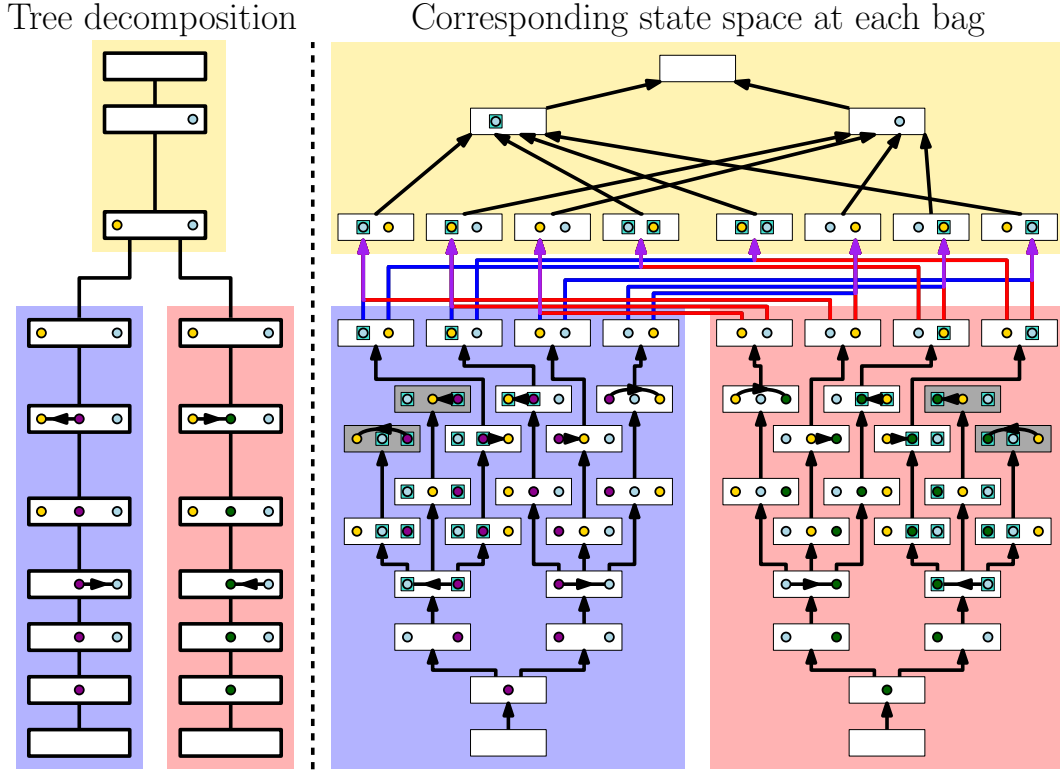
■ **Figure 9** An instance of a Restricted Feedback Morse Order (R-FMO) subproblem (left), together with two feasible solutions (right): two different feedback Morse orders on the same instance (top and bottom) inducing different sets of matched and unmatched vertices.

3.3 Dynamic program on a tree decomposition

We now describe the dynamic program at a high level; full recurrences and a formal DP invariant for R-FMO are deferred to Section A. For each bag t and each state (g, U) on X_t as above, we maintain a table entry $c[t, g, U]$, defined as the optimum of the R-FMO instance (G_t, X_t, g, U) , that is, the minimum total weight of unmatched vertices in $W_t \setminus X_t$ over all feedback Morse orders on G_t compatible with (g, U) ; if no such order exists, we set $c[t, g, U] = +\infty$. Figure 10 illustrates how such states are propagated along a tree decomposition and how locally invalid states are discarded. We process the nice tree decomposition bottom-up. At each bag type we update the table using only local information.

Leaf. The processed subgraph is empty, so there is a single state with empty order and empty matched set, and cost 0.

Introduce-vertex. A new vertex v enters the bag (and the graph) with no incident edges yet. It cannot already be matched, so $v \in U$ is forbidden. Otherwise we extend the order g by inserting v at its chosen position; the cost does not change.



■ **Figure 10** Dynamic program on the example from Figure 8. Bags of the tree decomposition are shown on the left; representative states (bag orders and matched subsets) on the right. States violating local adjacency, matching, or acyclicity constraints are discarded (grey).

Introduce-edge. A new edge (u, v) is introduced between vertices already in the bag. The order g determines whether it is forward or backward: (i) if (u, v) is forward in g , it can never be backward in any extension and thus can never enter the matching; (ii) if (u, v) is backward in g , it *must* be in the matching, and this is the unique place where it is introduced along the path. In the backward case we insist that u and v are currently unmatched in the child and become matched in the parent. Any state where this would create a double match in G_t is discarded.

Forget-vertex. A vertex v leaves the bag. At this moment all edges incident to v have already been introduced below, so v 's matching status is final. We branch on whether v is matched in the child: if v is unmatched, we add $\omega(v)$ to the cost; if v is matched, v never contributes again. We then take the minimum over all child states in which v appears at some position in the child order and the projected order on the remaining bag is g .

Join. Two subtrees with the same bag X_t are merged. The processed subgraph G_t is the union of G_s and $G_{s'}$, and the bag order g is the same in all three bags. The order g already decides which bag-internal edges are backward, and hence which bag vertices are forced to be matched via those edges; call this set $M_I(g)$. Every feasible state (g, U_\bullet) must satisfy $M_I(g) \subseteq U_\bullet$ for the parent and both children (if g induces conflicting backward edges, all such states are infeasible and $c[t, g, \cdot] = +\infty$). Outside $M_I(g)$, a bag vertex can be matched strictly below t in *at most one* of the two subtrees (there are no edges between the forgotten parts of the two subgraphs). Thus for a parent state (g, U_t) we look over all pairs of child matched sets $(U_s, U_{s'})$ such that $M_I(g) \subseteq U_s, U_{s'}, U_t$ and $U_t \setminus M_I(g) = (U_s \setminus M_I(g)) \dot{\cup} (U_{s'} \setminus M_I(g))$.

We then set $c[t, g, U_t]$ to the minimum of $c[s, g, U_s] + c[s', g, U_{s'}]$ over all such pairs.

A formal DP invariant and a proof of soundness and completeness of these transitions are deferred to Section A. At the root bag r , the bag is empty, so there is a single state (\emptyset, \emptyset) ; its value $c[r, \emptyset, \emptyset]$ is exactly the optimum of FMO on D , and hence of FMM and OMM.

3.4 Running time

We sketch the running-time bound; the full accounting is given in Appendix A.11. Let k be the treewidth of the underlying undirected graph of D and set $n := |V(D)|$. In a nice tree decomposition of width k , each bag has size at most $k+1$. A DP state is a pair (g, U) where g is a total order on the current bag and U is a subset of its vertices. Hence the number of states per bag is at most $(k+1)! \cdot 2^{k+1} \leq (k+1)^{k+1} \cdot 2^{k+1} = 2^{(k+1)\log_2(k+1)+(k+1)} = 2^{O(k \log k)}$. For each fixed state, leaf/introduce-vertex/introduce-edge transitions take $k^{O(1)}$ time, and a forget transition branches over $k+2$ insertion positions. At a join bag, the order g is shared by both children, and combining solutions amounts to splitting the bag-mask information between the two subtrees, yielding at most 2^{k+1} admissible child pairs per state. Thus the work per bag is $2^{O(k \log k)}$, and since the decomposition has $O(n)$ bags, the total running time is $2^{O(k \log k)} n$.

4 ETH-optimality

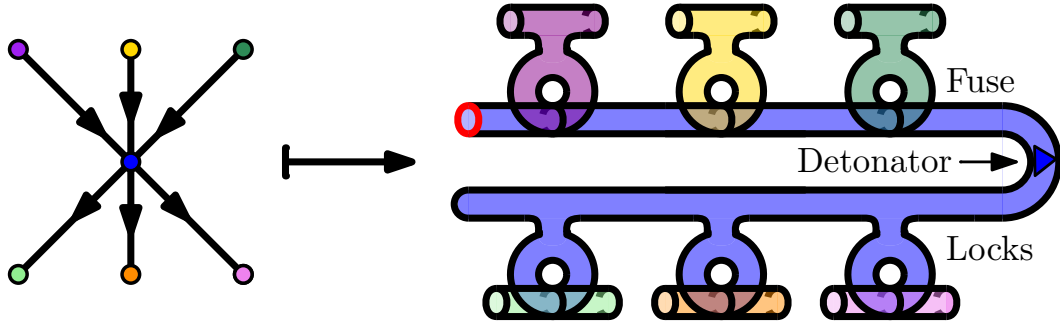
How expensive is treewidth for OMM? Our $2^{O(k \log k)} n$ -time algorithm shows what is achievable, and in this section we prove that this is indeed the true price under the Exponential Time Hypothesis (ETH). Starting from the ETH-based lower bound for DIRECTED FEEDBACK VERTEX SET (DFVS) parameterized by treewidth, we give a new polynomial-time reduction from DFVS to ERASIBILITY on 2-dimensional complexes of bounded coface degree. We then realize this reduction bag-by-bag using the Width Preserving Strategy (WiPS), which performs structural induction along a tree decomposition and keeps treewidth within a constant factor. As a consequence, any $2^{o(k \log k)} n^{O(1)}$ -time algorithm for OMM (even in this restricted setting) would yield such an algorithm for DFVS, contradicting ETH and pinning down the dependence on k as $2^{\Theta(k \log k)}$.

► **Theorem 13.** *Assuming ETH, ERASIBILITY parameterized by treewidth k admits no $2^{o(k \log k)} n^{O(1)}$ -time algorithm, even when the input is restricted to 2-dimensional simplicial complexes of top coface degree at most 4.*

4.1 Gadgets and obstructions

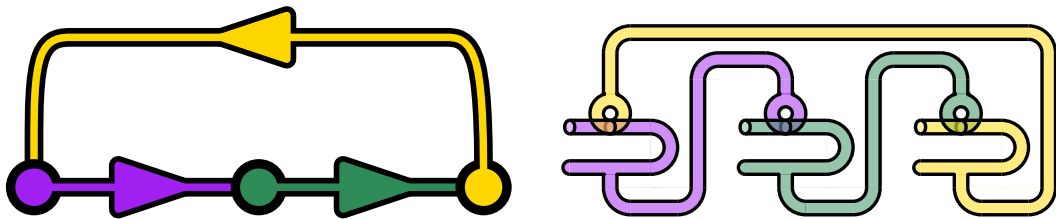
Vertex gadgets: fuses and locks. Let D be a DFVS instance. For each vertex $v \in V(D)$ we build a local gadget $Y^v = \mathcal{F}(v) \cup \mathcal{L}(v)$, illustrated in Figure 11. The fuse $\mathcal{F}(v)$ is a 2-dimensional simplicial complex homeomorphic to a hollow cylinder $S^1 \times I$ with two boundary circles: one is a free boundary circle (marked in red) from which we can start collapsing the complex, “unravelling” the fuse by elementary collapses along the cylinder; the other boundary circle is non-free and is glued to the lock $\mathcal{L}(v)$. The lock $\mathcal{L}(v)$ is a 2-dimensional simplicial complex homeomorphic to a compact orientable surface of genus $\deg^+(v)$ with a single boundary component, which is attached to this non-free boundary circle of the fuse. For each outgoing arc $v \rightarrow w$ in D , we select a distinct simple closed curve on $\mathcal{L}(v)$ and glue it to a cross-section circle of the fuse $\mathcal{F}(w)$, so that each such curve acts like a finger pinching the fuse: it prevents $\mathcal{F}(w)$ from collapsing past that cross-section as long as the lock $\mathcal{L}(v)$ is present. In the interior of $\mathcal{L}(v)$ we mark a single triangle $\text{deton}(v)$ (the

detonator); deleting this triangle makes the entire lock collapsible, eliminates all its pinches, and simultaneously releases every constraint that $\mathcal{L}(v)$ imposes on neighbouring fuses. We triangulate $\mathcal{L}(v)$ so that it becomes collapsible in either of two situations: after deleting $\text{deton}(v)$, or after its attached fuse $\mathcal{F}(v)$ has been completely collapsed. In particular, as long as $\text{deton}(v)$ is present and $\mathcal{F}(v)$ is intact, the lock cannot be collapsed while it still pinches some neighbouring fuse.



■ **Figure 11** Schematic vertex gadget for a vertex v : the fuse $\mathcal{F}(v)$ and the lock region $\mathcal{L}(v)$.

Ouroboroi as obstructions. Fix a directed cycle $C = (v_1, \dots, v_\ell)$ in D . For each arc (v_i, v_{i+1}) (indices modulo ℓ) we use one outgoing handle of $\mathcal{L}(v_i)$ and glue it so that it pinches the fuse $\mathcal{F}(v_{i+1})$ as described above. Taking exactly these pieces along the cycle yields a closed ring of vertex gadgets in which each lock pinches the next fuse; because of the visual similarity to a snake eating its own tail, we call such a ring an ℓ -*ouroboros*, see Figure 12. Along an ouroboros, each fuse can be collapsed from its free boundary until it reaches the first pinch, but it cannot be collapsed past that point while the corresponding lock is present. By construction, every edge in this ring belongs to at least two triangles (coming from the fuse, the lock, or their intersection), so inside this subcomplex there are no free edges and hence no elementary collapses. In particular, an ouroboros persists under any sequence of elementary collapses until at least one of its locks is destroyed, and we will use these rings as obstructions witnessing the presence of directed cycles in D .



■ **Figure 12** A directed 3-cycle in D and the corresponding 3-ouroboros: three vertex gadgets arranged in a ring, each lock pinching the next fuse. No edge on this ring is free, so it remains non-erasible until some detonator is deleted.

4.2 Correctness of the reduction

Let Y be the complex constructed from a DFVS instance D , and for each vertex v let $\text{deton}(v)$ be its detonator triangle in the gadget Y^v . We show that this construction yields a parameter-preserving polynomial-time reduction from DFVS to ERASIBILITY: for every

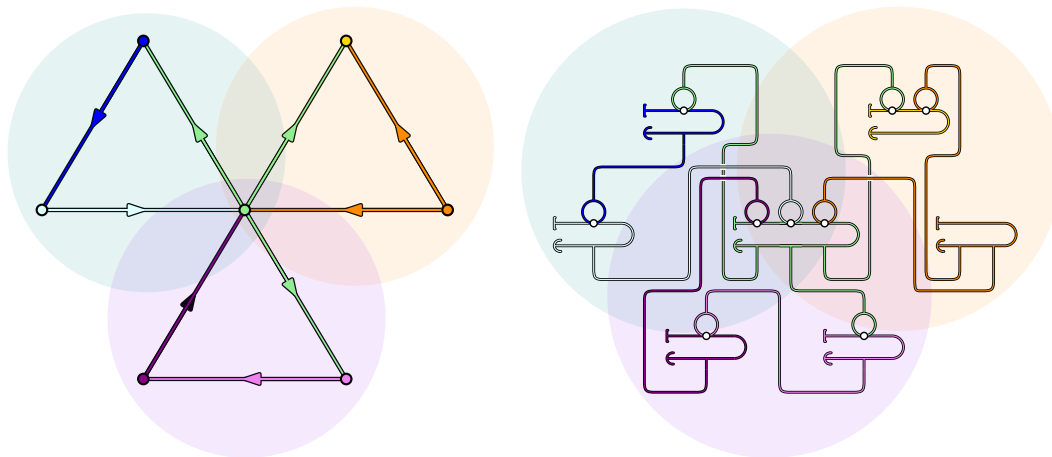
integer s , D has a feedback vertex set of size at most s if and only if Y becomes erasible after deleting at most s triangles.

Forward direction. Let $S \subseteq V(D)$ be a feedback vertex set of size at most s , and let $T := \{\text{deton}(v) \mid v \in S\}$. Deleting $\text{deton}(v)$ makes the entire lock $\mathcal{L}(v)$ collapsible and removes all its pinches on neighbouring fuses, so in $Y \setminus T$ we can collapse every lock $\mathcal{L}(v)$ with $v \in S$. Since $D \setminus S$ is acyclic, we can order its vertices topologically and, in that order, collapse each remaining gadget Y^v : once all incoming locks to $\mathcal{F}(v)$ have been removed, the fuse $\mathcal{F}(v)$ collapses completely, and by the gadget design the remaining lock $\mathcal{L}(v)$ then collapses as well. At the end only gadgets for vertices in S remain, but their locks have already been removed and their fuses are just cylinders with a free boundary, so they also collapse. Thus $Y \setminus T$ is erasible after deleting $|T| = |S| \leq s$ triangles.

Backward direction. Conversely, let T be a set of at most s triangles such that $Y \setminus T$ is erasible, and define $S' := \{v \in V(D) \mid Y^v \cap T \neq \emptyset\}$. Clearly $|S'| \leq |T| \leq s$. Suppose for contradiction that $D \setminus S'$ still contains a directed cycle $C = (v_1, \dots, v_\ell)$. By construction, the gadgets $Y^{v_1}, \dots, Y^{v_\ell}$ contain an ℓ -ouroboros subcomplex Z . Since no gadget in $Y \setminus T$ intersects T , Z is disjoint from T , and every edge of Z still lies in at least two triangles in $Y \setminus T$. Hence no edge of Z is ever free, so no sequence of elementary collapses can remove Z , and $Y \setminus T$ is not erasible—a contradiction. Thus $D \setminus S'$ is acyclic, and S' is a feedback vertex set of size at most s .

4.3 Preserving width via WiPS

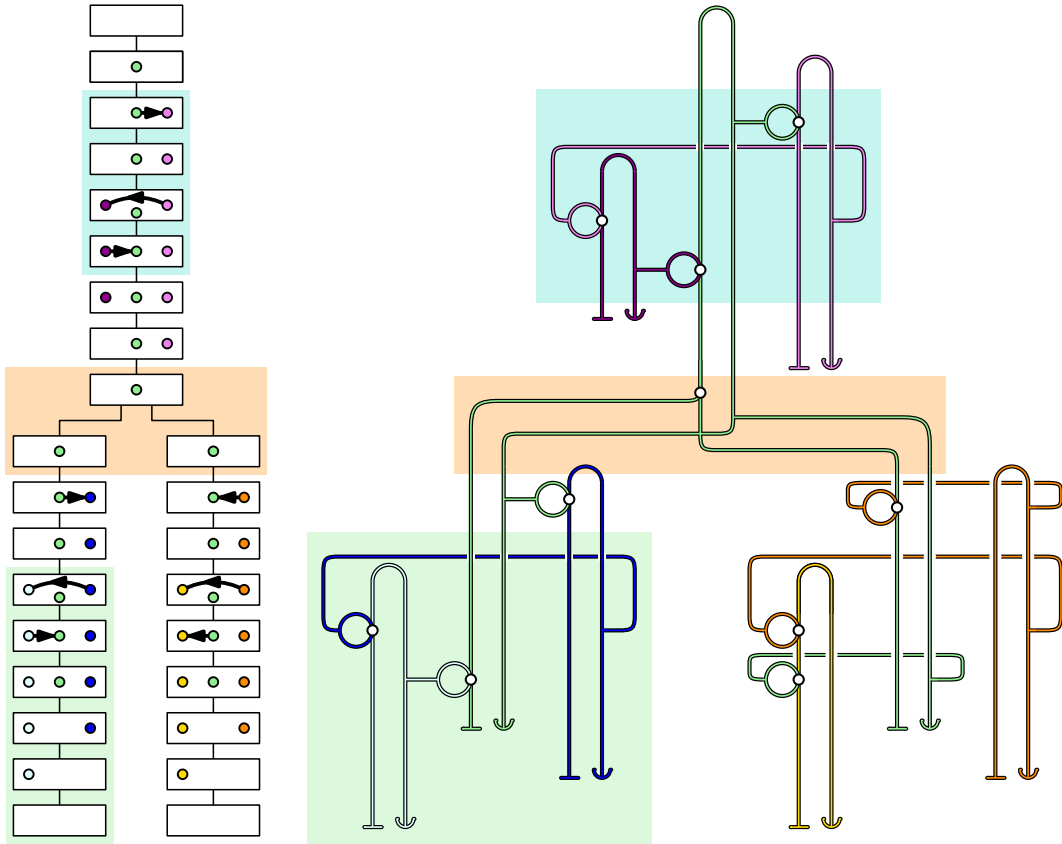
Width blow-up. Hardness reductions for problems parameterized by treewidth must control the width of the target instance: a naïve “glue all gadgets at once” construction can easily turn a bounded-treewidth graph into a complex whose Hasse diagram has very large treewidth. In our setting, globally attaching all vertex gadgets Y^v would allow long fuses and many handles to interact and form large grid-like regions in the Hasse diagram, even when D itself has small treewidth; see [5] for a concrete construction or Figure 13 for intuition.



■ **Figure 13** Naïve global gluing of all gadgets. The digraph (top) has small treewidth, but the assembled space (bottom) may develop large intertwined regions in the Hasse diagram, with no a priori width bound.

WiPS. To avoid this blow-up, we assemble the same gadgets *incrementally* along a nice tree decomposition of D , following the Width Preserving Strategy (WiPS) [42]. For each bag X_i we maintain a partial complex Y_i together with a small interface of boundary

circles associated with the vertices in X_t , and when moving from a child bag to its parent we only apply constant-size local updates touching this interface: at an introduce-vertex bag we attach a fresh gadget $\mathcal{F}(v) \cup \mathcal{L}(v)$; at an introduce-edge bag we add a single pinching handle between $\mathcal{L}(u)$ and $\mathcal{F}(v)$; at a forget-vertex bag we cap off the remaining boundary components of v ; and at a join bag we merge the two partial gadgets for each v along a constant-size interface (on the lock side via a pair-of-pants, on the fuse side by attaching both child cylinders to a common boundary circle and extending it by a short cylinder). Intuitively, each bag only “sees” a bounded portion of the complex, and only a bounded number of new simplices is introduced per bag; see Figure 14.



■ **Figure 14** WiPS-style construction. Left: a nice tree decomposition of the digraph in Figure 13. Right: the space is grown bag-by-bag, each bag exposing only a small interface and adding only constant-size pieces. This ensures that the Hasse diagram maintains treewidth $O(k)$.

Summary Instantiating WiPS with our gadgets, we obtain that if D has treewidth k , then the complex Y produced by the above construction has a Hasse diagram of treewidth at most $ck + c_0$ for fixed constants c, c_0 independent of D , and $|Y|$ remains polynomial in $|D|$. A detailed WiPS induction invariant and the exact bag-by-bag construction are deferred to Section B; in the main text we only use this width bound together with the gadget behavior described above. Together with the correctness of the DFVS-to-ERASIBILITY reduction proved above, this yields Theorem 13.

5 Discussion

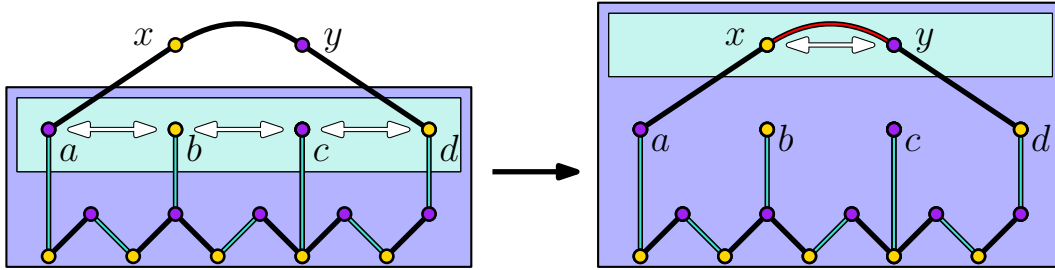
Table 1 summarises our treewidth-parameterized bounds. For FMM/FMO on digraphs, OMM on Hasse diagrams, and 2D ERASABILITY with coface degree at most 4 we obtain algorithms running in time $2^{O(k \log k)}n$, and our width-preserving reduction from DFVS shows that no $2^{o(k \log k)}n^{O(1)}$ algorithm exists under ETH. Thus these problems have optimal $2^{\Theta(k \log k)}n^{O(1)}$ dependence on treewidth. The rows with unknown ETH bounds in Table 1 show that the same dynamic programme extends to OMM on triangulated manifolds and to negative-weight FMM/FMO, and it remains open whether ETH lower bounds also carry over or whether the extra structure allows faster algorithms. Our algorithm also solves AC-FM on bipartite graphs, yielding a $2^{O(k \log k)}n^{O(1)}$ time bound. Since AC-FM coincides with URM [26], this also gives a $2^{O(k \log k)}n^{O(1)}$ algorithm for URM in the bipartite setting. By contrast, on general graphs the recent treewidth-based dynamic programme of [15] runs in $2^{O(k^2)}n^{O(1)}$ time. Our ETH lower bound already holds even for bipartite graphs of maximum degree at most 4, and in particular for the bipartite incidence graphs arising from 2-complexes. Whether the $2^{O(k \log k)}$ dependence can be achieved for general graphs remains open.

Problem	Setting	Algorithm	ETH
FMM/FMO	General digraphs, any weights	$2^{O(k \log k)}$	$2^{o(k \log k)}$
FMM/FMO	General digraphs, negative weights	$2^{O(k \log k)}$	–
OMM	DAGs/Hasse diagrams	$2^{O(k \log k)}$	$2^{o(k \log k)}$
OMM	Triangulated d -manifolds	$2^{O(k \log k)}$	–
2D ERASABILITY	Coface degree ≤ 4 , unweighted	$2^{O(k \log k)}$	$2^{o(k \log k)}$
<i>Conjectured</i> \rightarrow	Coface degree ≤ 3 , embeddable in \mathbb{R}^3	$2^{O(k \log k)}$	$2^{o(k \log k)}$
AC-FM/URM	General graphs, algorithm from [15]	$2^{O(k^2)}$	$2^{o(k \log k)}$
AC-FM/URM	Bipartite graphs	$2^{O(k \log k)}$	$2^{o(k \log k)}$
AC-FM/URM	Bipartite graphs, maximum degree ≤ 4	$2^{O(k \log k)}$	$2^{o(k \log k)}$

■ **Table 1** Upper and lower running-time bounds in the treewidth parameter k for the problems considered in this paper, suppressing polynomial factors in n . The first block contains the problems we study explicitly, ordered from more general to more restricted settings. The bottom block records bounds for AC-FM/URM; the bounded-degree row indicates that the ETH lower bound already holds for bipartite incidence graphs arising from 2D ERASABILITY.

Representation matters. Forman’s correspondence identifies discrete Morse matchings with Morse functions or orders on the underlying Hasse diagram, but these viewpoints behave very differently for treewidth-based algorithms. Most prior work, including Hasse-based formulations of OMM and the parameterized algorithm of [12], stays in the matching language: discrete gradients are matchings and gradient paths are alternating paths. In that setting one either appeals to meta-theorems such as Courcelle’s theorem, with non-elementary state spaces, or designs ad-hoc state summaries based on alternating-path patterns on each bag of a tree decomposition. Figure 15 shows that such summaries are delicate: alternating reachability is not transitive, and merging states solely on the basis of their alternating pattern can silently discard globally optimal extensions. In particular, our example suggests that the union–find based invariant used in [12], which implicitly treats alternating connectivity as an equivalence relation, is too coarse as stated; one really needs to know which vertices are alternating-reachable from which, not just which “components” they lie in. The recent

AC-FM/URM dynamic program of [15] can be seen as a systematic matching-based repair: on each bag it stores an “alternating matrix” recording, for every pair of vertices, whether they are connected by an alternating path with respect to the current matching, that is, the full relation $R_M \subseteq B \times B$ of alternating reachability. This avoids over-pruning and, on bipartite incidence graphs (such as spines or Hasse diagrams), yields a faithful matching-based implementation of discrete Morse matchings, but at the price of a $2^{\Theta(k^2)}$ state space for bags of size $O(k)$, as reflected in Table 1. Beyond the bipartite/Hasse case the relationship between AC-FM and FMM breaks down, and we do not currently see how to compress alternating information on general graphs to obtain a $2^{O(k \log k)}$ dependence without a substantially different representation.



■ **Figure 15** Summaries based only on alternating-path patterns can over-prune. **Left:** the DP merges states whenever the alternating-path pattern on the current bag is the same; in particular, states that differ only in how they treat a and d are identified. **Right:** after introducing x, y , the matching $\{ax, yd\}$ is a valid extension and can be arranged to be uniquely optimal, but no surviving state represents it, because all states that kept a and d separate were merged earlier.

Conclusion. We give an order-based dynamic program for OPTIMAL MORSE MATCHING on bounded-treewidth complexes with running time $2^{O(k \log k)}n$ and, via WiPS-style width-preserving reductions, ETH-tight lower bounds that persist even under strong restrictions on the input. For discrete Morse theory, our results suggest that for treewidth, taking the path of functions and orderings has made all the difference. Looking ahead, the road keeps going:

- **Three gaps suggested by Table 1.** First, prove the conjectured ETH-tight lower bound for 2D ERASABILITY on complexes of coface degree ≤ 3 embeddable in \mathbb{R}^3 . Second, for triangulated manifolds can we obtain a $2^{O(k)}n^{O(1)}$ -time algorithm for OMM? Third, for AC-FM/URM we have an ETH-tight $2^{\Theta(k \log k)}n^{O(1)}$ running time on bipartite graphs, while on general graphs the best known DP runs in $2^{O(k^2)}n^{O(1)}$ time [15]. Can we show under ETH that a quadratic dependence on treewidth in the exponent is unavoidable in the general-graph case?
- **A locality constraint for OMM.** With solution-size parameterizations remaining W[P]-hard [12, 4], it is natural to look for complementary structural parameters. One concrete direction is to enforce *local* simplification by bounding (or minimizing) the length of the longest gradient path, equivalently the longest alternating path in the Hasse diagram after reversing matched edges. What is the complexity of OMM under such a locality constraint, and how does it interact with bounded treewidth?
- **WiPS beyond this paper.** Our ETH lower bound relies on the Width Preserving Strategy (WiPS) [42], which enables reductions to be carried out bag-by-bag while keeping treewidth under control. Can WiPS be developed into a general toolbox for proving tight treewidth lower bounds (and perhaps transferring XNLP-hardness) for other problems studied via treewidth in topology and geometry, for example quantum invariants and

decision problems on triangulations [10, 13, 6]?

References

- 1 Madjid Allili, Tomasz Kaczynski, Claudia Landi, and Filippo Masoni. Acyclic partial matchings for multidimensional persistence: Algorithm and combinatorial interpretation. *Journal of Mathematical Imaging and Vision*, 61(2):174–192, 2019. doi:10.1007/s10851-018-0843-8.
- 2 Ulrich Bauer, Carsten Lange, and Max Wardetzky. Optimal topological simplification of discrete functions on surfaces. *Discrete & Computational Geometry*, 47(2):347–377, 2012. doi:10.1007/s00454-011-9350-z.
- 3 Ulrich Bauer and Abhishek Rathod. Hardness of approximation for Morse matching. In Timothy M. Chan, editor, *Proceedings of the Thirtieth Annual ACM-SIAM Symposium on Discrete Algorithms, SODA 2019, San Diego, California, USA, January 6-9, 2019*, pages 2663–2674. SIAM, 2019. doi:10.1137/1.9781611975482.165.
- 4 Ulrich Bauer and Abhishek Rathod. Parameterized inapproximability of Morse matching. *Computational Geometry*, 126:102148, 2025. doi:10.1016/j.comgeo.2024.102148.
- 5 Mitchell Black, Nello Blaser, Amir Nayyeri, and Erlend Raa Vågset. ETH-tight algorithms for finding surfaces in simplicial complexes of bounded treewidth. In *38th International Symposium on Computational Geometry (SoCG 2022)*, volume 224 of *Leibniz International Proceedings in Informatics (LIPIcs)*, pages 17:1–17:16. Schloss Dagstuhl – Leibniz-Zentrum für Informatik, 2022. doi:10.4230/LIPIcs.SocG.2022.17.
- 6 Mitchell Black and Amir Nayyeri. Finding minimum bounded and homologous chains in simplicial complexes with bounded-treewidth 1-skeleton. arXiv, 2021. arXiv:2107.10339.
- 7 Nello Blaser, Morten Brun, Lars M. Salbu, and Erlend Raa Vågset. The parameterized complexity of finding minimum bounded chains. *Computational Geometry*, 122:102102, 2024. doi:10.1016/j.comgeo.2024.102102.
- 8 Nello Blaser and Erlend Raa Vågset. Homology localization through the looking-glass of parameterized complexity theory. *Journal of Applied and Computational Topology*, 9:16, 2025. doi:10.1007/s41468-025-00212-0.
- 9 Marthe Bonamy, Łukasz Kowalik, Jesper Nederlof, Michał Pilipczuk, Arkadiusz Socała, and Marcin Wrochna. On directed feedback vertex set parameterized by treewidth. In Andreas Brandstädt, Ekkehard Köhler, and Klaus Meer, editors, *Graph-Theoretic Concepts in Computer Science (WG 2018)*, volume 11159 of *Lecture Notes in Computer Science*, pages 65–78. Springer, 2018. Also available as arXiv:1707.01470. doi:10.1007/978-3-030-00256-5_6.
- 10 Benjamin A. Burton. The HOMFLY-PT Polynomial is Fixed-Parameter Tractable. In Bettina Speckmann and Csaba D. Tóth, editors, *34th International Symposium on Computational Geometry (SoCG 2018)*, volume 99 of *Leibniz International Proceedings in Informatics (LIPIcs)*, pages 18:1–18:14, Dagstuhl, Germany, 2018. Schloss Dagstuhl – Leibniz-Zentrum für Informatik. doi:10.4230/LIPIcs.SocG.2018.18.
- 11 Benjamin A. Burton and Rodney G. Downey. Courcelle’s theorem for triangulations. *Journal of Combinatorial Theory, Series A*, 146:264–294, February 2017. doi:10.1016/j.jcta.2016.10.001.
- 12 Benjamin A. Burton, Thomas Lewiner, João Paixão, and Jonathan Spreer. Parameterized complexity of discrete Morse theory. *ACM Transactions on Mathematical Software*, 42(1):6:1–6:24, March 2016. doi:10.1145/2738034.
- 13 Benjamin A. Burton, Clément Maria, and Jonathan Spreer. Algorithms and complexity for Turaev–Viro invariants. *Journal of Applied and Computational Topology*, 2(1-2):33–53, 2018. doi:10.1007/s41468-018-0016-2.
- 14 Frédéric Cazals, Frédéric Chazal, and Thomas Lewiner. Molecular shape analysis based upon the Morse–Smale complex and the Connolly function. In *Proceedings of the 19th Annual Symposium on Computational Geometry*, pages 351–360, 2003. doi:10.1145/777792.777845.

- 15 Juhi Chaudhary, Ignasi Sau, and Meirav Zehavi. A parameterized perspective on uniquely restricted matchings. *Procedia Computer Science*, 273:509–516, 2025. Also available as arXiv:2508.12004. doi:10.1016/j.procs.2025.10.339.
- 16 Justin Curry, Robert Ghrist, and Vidit Nanda. Discrete Morse theory for computing cellular sheaf cohomology. *Foundations of Computational Mathematics*, 16(4):875–897, 2016. doi:10.1007/s10208-015-9266-8.
- 17 Marek Cygan, Fedor V. Fomin, Łukasz Kowalik, Daniel Lokshantov, Dániel Marx, Marcin Pilipczuk, Michał Pilipczuk, and Saket Saurabh. *Parameterized Algorithms*. Springer, Cham, 2015. doi:10.1007/978-3-319-21275-3.
- 18 Olaf Delgado-Friedrichs, Vanessa Robins, and Adrian Sheppard. Skeletonization and partitioning of digital images using discrete Morse theory. *IEEE Transactions on Pattern Analysis and Machine Intelligence*, 37(3):654–666, 2015. doi:10.1109/TPAMI.2014.2346172.
- 19 Rodney G. Downey and Michael R. Fellows. *Parameterized Complexity*. Monographs in Computer Science. Springer, New York, NY, 1999. doi:10.1007/978-1-4612-0515-9.
- 20 Michael Farber. *Invitation to Topological Robotics*. Zurich Lectures in Advanced Mathematics. European Mathematical Society (EMS), Zürich, 2008. doi:10.4171/054.
- 21 Robin Forman. Morse theory for cell complexes. *Advances in Mathematics*, 134(1):90–145, 1998. doi:10.1006/aima.1997.1650.
- 22 Robin Forman. A user’s guide to discrete Morse theory. *Séminaire Lotharingien de Combinatoire*, 48:B48c, 2002. URL: <https://www.mat.univie.ac.at/~slc/wpapers/s48forman.html>.
- 23 Ulderico Fugacci, Federico Iuricich, and Leila De Florian. Computing discrete Morse complexes from simplicial complexes. *Graphical Models*, 103:101023, 2019. doi:10.1016/j.gmod.2019.101023.
- 24 Robert Ghrist. Configuration spaces, braids, and robotics. In *Braids: Introductory Lectures on Braids, Configurations and Their Applications*, pages 263–304. World Scientific, 2010. doi:10.1142/9789814291415_0004.
- 25 Xavier Goaoc, Pavel Paták, Zuzana Patáková, Martin Tancer, and Uli Wagner. Shellability is NP-complete. *Journal of the ACM*, 66(3):21, 2019. doi:10.1145/3314024.
- 26 Martin Charles Golumbic, Tom Hirst, and Michael Lewenstein. Uniquely restricted matchings. *Algorithmica*, 31(2):139–154, 2001. doi:10.1007/s00453-001-0004-z.
- 27 Shaun Harker, Konstantin Mischaikow, Marian Mrozek, and Vidit Nanda. Discrete Morse theoretic algorithms for computing homology of complexes and maps. *Foundations of Computational Mathematics*, 14(1):151–184, 2014. doi:10.1007/s10208-013-9145-0.
- 28 Kristóf Huszár and Jonathan Spreer. 3-Manifold Triangulations with Small Treewidth. In Gill Barequet and Yusu Wang, editors, *35th International Symposium on Computational Geometry (SoCG 2019)*, volume 129 of *Leibniz International Proceedings in Informatics (LIPIcs)*, pages 44:1–44:20, Dagstuhl, Germany, 2019. Schloss Dagstuhl – Leibniz-Zentrum für Informatik. doi:10.4230/LIPIcs.SocG.2019.44.
- 29 Kristóf Huszár and Jonathan Spreer. On the width of complicated JSJ decompositions. *Discrete & Computational Geometry*, 74(4):917–943, 2025. doi:10.1007/s00454-025-00746-1.
- 30 Kristóf Huszár, Jonathan Spreer, and Uli Wagner. On the treewidth of triangulated 3-manifolds. *Journal of Computational Geometry*, 10(2):70–98, 2019. doi:10.20382/jocg.v10i2a5.
- 31 Russell Impagliazzo, Ramamohan Paturi, and Francis Zane. Which problems have strongly exponential complexity? *Journal of Computer and System Sciences*, 63(4):512–530, 2001. doi:10.1006/jcss.2001.1774.
- 32 Michael Joswig and Marc E. Pfetsch. Computing optimal Morse matchings. *SIAM Journal on Discrete Mathematics*, 20(1):11–25, 2006. doi:10.1137/S0895480104445885.
- 33 Harish Kannan, Emil Saucan, Indrava Roy, and Areejit Samal. Persistent homology of unweighted complex networks via discrete Morse theory. *Scientific Reports*, 9:13817, 2019. doi:10.1038/s41598-019-50202-3.

- 34 Thomas Lewiner, Helio Lopes, and Geovan Tavares. Toward optimality in discrete Morse theory. *Experimental Mathematics*, 12(3):271–285, 2003. doi:10.1080/10586458.2003.10504498.
- 35 Thomas Lewiner, Helio Lopes, and Geovan Tavares. Applications of Forman’s discrete Morse theory to topology visualization and mesh compression. *IEEE Transactions on Visualization and Computer Graphics*, 10(5):499–508, 2004. doi:10.1109/TVCG.2004.18.
- 36 Rémy Malgouyres and Angel R. Francés. Determining whether a simplicial 3-complex collapses to a 1-complex is NP-complete. In *Discrete Geometry for Computer Imagery (DGCI 2008)*, volume 4992 of *Lecture Notes in Computer Science*, pages 177–188. Springer, 2008. doi:10.1007/978-3-540-79126-3_17.
- 37 Marston Morse. *The Calculus of Variations in the Large*, volume 18 of *American Mathematical Society Colloquium Publications*. American Mathematical Society, Providence, RI, 1996. Reprint of the 1934 original. doi:10.1090/coll/018.
- 38 Soham Mukherjee. Denoising with discrete Morse theory. *The Visual Computer*, 37(9):2883–2894, 2021. doi:10.1007/s00371-021-02255-7.
- 39 Abhishek Rathod, Talha Bin Masood, and Vijay Natarajan. Approximation algorithms for Max Morse Matching. *Computational Geometry*, 61:1–23, 2017. doi:10.1016/j.comgeo.2016.10.002.
- 40 Nicholas A. Scoville. *Discrete Morse Theory*, volume 90 of *Student Mathematical Library*. American Mathematical Society, Providence, RI, 2019. doi:10.1090/stml/090.
- 41 Martin Tancer. Recognition of collapsible complexes is NP-complete. *Discrete & Computational Geometry*, 55(1):21–38, 2016. doi:10.1007/s00454-015-9747-1.
- 42 Erlend Raa Vågset. *Optimal parameterized algorithms for solving NP-hard problems in topology*. PhD thesis, University of Bergen, Bergen, Norway, 2024. URL: https://urn.nb.no/URN:NBN:no-nb_pliktmonografi_000039725.

A Algorithm Details

We prove that the dynamic program from Section 3 correctly computes the minimum possible total weight of unmatched vertices in a feedback Morse order. The proof is by induction over a rooted nice tree decomposition of the underlying undirected graph of the input digraph D , processed bottom-up. We begin by fixing notation for tree decompositions and the introduce-edge refinement used to define the processed subgraphs G_t .

A.1 Nice tree decompositions and introduce-edge nodes

For completeness, we recall (rooted) nice tree decompositions and the introduce-edge refinement used by the dynamic program; see e.g. [17].

► **Definition 14** (Tree decomposition). *A tree decomposition of an undirected graph $G = (V, E)$ is a pair $(T, \{X_t\}_{t \in V(T)})$, where T is a tree and each $X_t \subseteq V$ is a bag, such that:*

1. $\bigcup_{t \in V(T)} X_t = V$.
2. for each $\{u, v\} \in E$ there exists t with $\{u, v\} \subseteq X_t$.
3. for each $v \in V$, the set $\{t \in V(T) : v \in X_t\}$ induces a connected subtree of T .

The width of the decomposition is $\max_t |X_t| - 1$.

► **Definition 15** (Rooted nice tree decomposition). *Fix a root $r \in V(T)$ and orient T away from r . A rooted tree decomposition is nice if every node is of one of the following types:*

- **Leaf:** no children.
- **Introduce-vertex:** one child s with $X_t = X_s \cup \{v\}$.
- **Forget-vertex:** one child s with $X_t = X_s \setminus \{v\}$.
- **Join:** two children s, s' with $X_t = X_s = X_{s'}$.

It is standard that we may assume the decomposition is given in rooted nice form without increasing the width. We also use the standard further refinement that inserts unary *introduce-edge* nodes (with unchanged bags) so that each edge is introduced at some introduce-edge node whose bag contains both endpoints, and along any root-to-node path each edge is introduced at most once. These refinements can be carried out efficiently and increase the number of bags only by a linear factor.

A.2 Feedback Morse orders and induced matchings

We next recall the order-based formulation and the induced set of backward edges used throughout the DP and its correctness proof.

Given a digraph $D = (V, E)$ and a total order $\pi = (v_1, \dots, v_n)$ of V , we call an edge $(u, v) \in E$ *backward* with respect to π if v appears before u in π . We write

$$M(\pi) := \{(u, v) \in E : (u, v) \text{ is backward with respect to } \pi\},$$

so $M(\pi)$ is the set of all backward edges of D with respect to π .

► **Definition 16** (Feedback Morse order). *Let $D = (V, E)$ be a digraph. A total order π of V is a feedback Morse order if the set $M(\pi)$ of backward edges is a matching (no two edges in $M(\pi)$ share a vertex).*

The crucial observation is that once we fix π , the matching is *forced* to be $M(\pi)$; and for such an induced matching, the edge-reversed digraph $D_{M(\pi)}$ is always acyclic.

► **Lemma 17** (Order-induced DAG). *Let $D = (V, E)$ be a digraph and let π be any total order of V . Define $M(\pi)$ as above and let $D_{M(\pi)}$ be the digraph obtained from D by reversing all edges in $M(\pi)$. Then every edge of $D_{M(\pi)}$ points forward with respect to π , and in particular $D_{M(\pi)}$ is acyclic.*

Proof. Let $(u, v) \in E$. If $(u, v) \notin M(\pi)$, then it is forward with respect to π , and we do not reverse it; in $D_{M(\pi)}$ we still have $u \rightarrow v$ with u before v in π . If $(u, v) \in M(\pi)$, then it is backward with respect to π , so v appears before u ; we reverse it to $v \rightarrow u$, which again points from an earlier to a later vertex in π . Thus every edge of $D_{M(\pi)}$ points forward in π , so π is a topological order of $D_{M(\pi)}$ and $D_{M(\pi)}$ is acyclic. ◀

Combining this with the definition of feedback Morse matchings (Problem 8) yields the following correspondence between matchings and orders.

► **Corollary 18** (Matchings vs. orders). *Let $D = (V, E)$ be a digraph.*

- *If π is a feedback Morse order, then $M(\pi)$ is a feedback Morse matching on D , and $(\pi, M(\pi))$ is a feedback Morse pair.*
- *Conversely, if $M \subseteq E$ is a feedback Morse matching, then there exists a total order π such that $M(\pi) = M$; in particular π is a feedback Morse order.*

Proof. If π is a feedback Morse order, then by definition $M(\pi)$ is a matching, and by Lemma 17 the digraph $D_{M(\pi)}$ is acyclic. Thus $M(\pi)$ is a feedback Morse matching and $(\pi, M(\pi))$ is a feedback Morse pair.

Conversely, if M is a feedback Morse matching then D_M is acyclic and admits a topological order π . For every edge $(u, v) \in M$, the reversed edge (v, u) lies in D_M and must point forward with respect to π , so v appears before u and (u, v) is backward with respect to π . For every edge $(u, v) \notin M$, the edge is not reversed and appears as (u, v) in D_M ; since π is a topological order, u must appear before v , so (u, v) is forward with respect to π . Hence the set of backward edges with respect to π is precisely M , that is, $M(\pi) = M$. Since M is a matching, $M(\pi)$ is a matching and π is a feedback Morse order. ◀

In particular, every feedback Morse matching arises from at least one feedback Morse order π , and for such an order the matching is uniquely determined as $M(\pi)$. This justifies working purely with orders: the objective value for FMM on D can be computed from any feedback Morse order by considering the induced matching $M(\pi)$.

A.3 R-FMO, processed subgraphs, and the DP invariant

We use the Restricted Feedback Morse Order (R-FMO) subproblem defined in Section 3.2 (Problem 12). For convenience, we recall it informally in the order-based viewpoint.

For a digraph G with vertex set W , a subset $X \subseteq W$, a total order g on X , and a subset $U \subseteq X$, we consider all feedback Morse orders π on G such that:

- the restriction of π to X equals the prescribed order g ;
- the vertices of X that are incident to some backward edge in $M(\pi)$ are exactly the set U , i.e.,

$$U = V(M(\pi)) \cap X,$$

where $M(\pi)$ is the set of backward edges of G with respect to π .

Among all such π , the R-FMO value is the minimum total weight of unmatched vertices in $W \setminus X$, that is

$$\sum_{\substack{v \in W \setminus X \\ v \notin V(M(\pi))}} \omega(v).$$

In the dynamic program, for each bag t of the nice tree decomposition we let W_t be the set of vertices that appear in the subtree rooted at t . We define G_t to be the *processed subgraph* of D whose vertex set is W_t and whose edge set consists exactly of those edges whose introduce-edge bags lie in this subtree. We rely on an *edge introduction discipline*, informally meaning that each edge is introduced at most once along each root-to-node path (see (T2) in Section A.4). In particular, every edge with both endpoints in a join bag appears in both child subtrees, and by the time a vertex v is forgotten, all edges incident to v have been introduced below its forget-vertex bag.

The bag at t is X_t . For a state (g, U) at t (a total order g on X_t and a subset $U \subseteq X_t$) we define $c[t, g, U]$ to be the optimum value of the R-FMO instance (G_t, X_t, g, U) in the above sense.

DP invariant. For every bag t and state (g, U) on X_t , the DP value $c[t, g, U]$ equals the minimum total weight of vertices in $W_t \setminus X_t$ that are unmatched under some feedback Morse order π on G_t such that:

- the restriction of π to X_t is the order g ;
- the vertices of X_t that are incident to backward edges in $M(\pi)$ are exactly the set U , i.e.,

$$U = V(M(\pi)) \cap X_t.$$

If no such feedback Morse order exists on G_t , we set $c[t, g, U] = +\infty$.

We prove by induction on the structure of the nice tree decomposition that this invariant holds for every bag. At the root (whose bag is empty) there is a single state (\emptyset, \emptyset) , and by the invariant its value is the global optimum of FMO (and hence of FMM by Corollary 18).

A.4 Tree-decomposition assumptions

We use the following properties of the refined nice tree decomposition of the underlying undirected graph of D . The refinement consists of adding introduce-edge bags as described earlier; the underlying vertex bags form a standard nice tree decomposition.

- (T1) *Running intersection.* For each vertex v , the set of bags containing v induces a connected subtree.
- (T2) *Edge introduction discipline (per path).* For each directed edge $(u, v) \in E(D)$ there is at least one introduce-edge bag whose vertex set contains both u and v . Along any root-to-node path in the tree decomposition, the edge (u, v) is introduced in at most one bag on that path.
- (T3) *Forget-after-edges.* For each vertex v , there is a unique forget-vertex bag at which v is removed from the bags. All introduce-edge bags that contain v lie strictly below this forget-vertex bag; above that bag, no introduce-edge bag contains v .
- (T4) *Join separation.* If t is a join bag with children s, s' , then $W_s \cap W_{s'} = X_t$, where W_s (resp. $W_{s'}$) is the set of vertices that appear in the subtree rooted at s (resp. s'). Moreover, there is no edge of D whose one endpoint lies in $W_s \setminus X_t$ and the other in $W_{s'} \setminus X_t$.

- (T5) *Bag-internal edges at joins.* If t is a join bag with children s, s' and $(u, v) \in E(D)$ satisfies $\{u, v\} \subseteq X_t$, then (u, v) is introduced in both subtrees: there is an introduce-edge bag for (u, v) in the subtree rooted at s and an introduce-edge bag for (u, v) in the subtree rooted at s' . Equivalently, every such edge (u, v) belongs to both processed subgraphs G_s and $G_{s'}$.

Property (T1) is the usual running-intersection condition for tree decompositions. Property (T4) is the standard separator property implied by (T1) on the underlying undirected graph. Properties (T2), (T3), and (T5) are enforced by our refinement with introduce-edge bags and capture our edge introduction discipline: edges are introduced as soon as possible, never twice along a single root-to-node path, and any edge whose endpoints lie in a join bag is present (and enforced) in both subtrees of that join.

A.5 Leaf bag

Let t be a leaf bag, so that $X_t = \emptyset$ and G_t is empty. The DP defines a single state $(g, U) = (\emptyset, \emptyset)$ with $c[t, \emptyset, \emptyset] = 0$.

Soundness. Since G_t has no vertices and no edges, there is exactly one feedback Morse order on G_t , namely the empty order. No vertex is unmatched (there are no vertices), so the true optimum value of the corresponding R-FMO instance is 0. Thus the DP value does not underestimate the optimum.

Completeness. Every feasible solution (here, just the empty order) is represented by this unique state (\emptyset, \emptyset) and has cost 0, so the DP value does not overestimate the optimum.

Hence the DP invariant holds at leaf bags.

A.6 Introduce-vertex bag

Let t be an introduce-vertex bag with child s , introducing a vertex v . Then $X_t = X_s \cup \{v\}$, and by (T3) no edge incident to v has an introduce-edge bag below t . In particular, the processed subgraph is $G_t = G_s \cup \{v\}$, and v is isolated in G_t .

For each state (g', U_t) on X_t , let g be the restriction of g' to X_s . The recurrence says:

$$c[t, g', U_t] = \begin{cases} +\infty, & \text{if } v \in U_t, \\ c[s, g, U_t \cap X_s], & \text{otherwise.} \end{cases}$$

Soundness.

If $v \in U_t$, then by the DP invariant v must be incident to some edge in the induced matching $M(\pi)$ for any feedback Morse order π on G_t consistent with (g', U_t) , that is, $v \in V(M(\pi)) \cap X_t = U_t$. But no edge incident to v lies in G_t , so no such matching edge exists; hence there is no feasible feedback Morse order π on G_t consistent with (g', U_t) , and the correct value is $+\infty$.

If $v \notin U_t$, take any feedback Morse order π_s on G_s that realises $c[s, g, U_t \cap X_s]$. Extend π_s to a total order π_t on G_t by inserting v in any position such that the induced order on X_t is exactly g' . Since v has no incident edges in G_t , the set of backward edges and hence the matching $M(\pi_t)$ are the same as in π_s . In particular,

$$V(M(\pi_t)) \cap X_s = V(M(\pi_s)) \cap X_s = U_t \cap X_s,$$

and $v \notin V(M(\pi_t))$, so $V(M(\pi_t)) \cap X_t = U_t$. Thus π_t is a feedback Morse order on G_t consistent with the state (g', U_t) .

Moreover, the set of vertices outside the bag does not change when we introduce v :

$$W_t \setminus X_t = W_s \setminus X_s,$$

and the unmatched vertices in $W_t \setminus X_t$ under π_t are exactly those in $W_s \setminus X_s$ under π_s , with the same weights. Hence the cost realised by π_t is exactly $c[s, g, U_t \cap X_s]$. The DP value in the second case is therefore achievable and does not underestimate the optimum.

Completeness.

Conversely, let π_t be any feedback Morse order on G_t consistent with (g', U_t) . Since v is isolated in G_t , it is unmatched under π_t , so $v \notin V(M(\pi_t))$. As $U_t = V(M(\pi_t)) \cap X_t$ by consistency, this implies $v \notin U_t$, so we are in the second case of the recurrence.

Restrict π_t to G_s , obtaining a feedback Morse order π_s on G_s whose restriction to X_s is g . The induced matching on G_s is just the restriction of $M(\pi_t)$, so

$$V(M(\pi_s)) \cap X_s = V(M(\pi_t)) \cap X_s = U_t \cap X_s.$$

No vertices are forgotten at t , so $W_s \setminus X_s = W_t \setminus X_t$, and the unmatched vertices in $W_s \setminus X_s$ under π_s are exactly those in $W_t \setminus X_t$ under π_t , with the same weights.

By the inductive hypothesis applied at s , the total weight of unmatched vertices in $W_s \setminus X_s$ under π_s is at least $c[s, g, U_t \cap X_s]$. Since the recurrence sets $c[t, g', U_t] = c[s, g, U_t \cap X_s]$, the cost of π_t is at least the DP value $c[t, g', U_t]$. Thus the DP does not overestimate the optimum for state (g', U_t) .

Therefore the DP invariant holds at introduce-vertex bags.

A.7 Introduce-edge bag

Let t be an introduce-edge bag with child s , introducing a single directed edge (u, v) . Then $X_t = X_s$, and the processed subgraph G_t is obtained from G_s by adding the edge (u, v) : they have the same vertex set, and the edge set of G_t is the edge set of G_s plus (u, v) . For each state (g, U_t) on X_t , write $u <_g v$ if u appears before v in g .

The recurrence says:

$$c[t, g, U_t] = \begin{cases} c[s, g, U_t], & \text{if } u <_g v, \\ c[s, g, U_t \setminus \{u, v\}], & \text{if } v <_g u \text{ and } \{u, v\} \subseteq U_t, \\ +\infty, & \text{otherwise.} \end{cases}$$

Soundness.

Consider the three cases.

(i) $u <_g v$. In any feedback Morse order π on G_t whose restriction to X_t is g , we must have u before v (the relative order of bag vertices is fixed), so (u, v) is forward with respect to π and does not belong to $M(\pi)$. Therefore the matching $M(\pi)$ and the set of unmatched vertices in $W_t \setminus X_t$ are the same as for any feedback Morse order on G_s with boundary state (g, U_t) . Thus the optimum cost at t equals that at s , and the recurrence is sound in this case.

(ii) $v <_g u$ and $\{u, v\} \subseteq U_t$. Then for any feedback Morse order π consistent with (g, U_t) we must have v before u in π , so the new edge (u, v) is backward with respect to π . By definition, $M(\pi)$ contains *all* backward edges, so $(u, v) \in M(\pi)$ and both endpoints u and v are matched.

On the current root-to- t path, the edge (u, v) is introduced for the first time at t by (T2), so $(u, v) \notin E(G_s)$. In particular, the only matching edge in $M(\pi)$ incident to either u or v is (u, v) itself. Hence, in the restriction of π to G_s , both u and v are unmatched. This means that in the child instance the matched bag vertices are exactly

$$U_s = U_t \setminus \{u, v\}.$$

Conversely, take any feedback Morse order π_s on G_s that realises $c[s, g, U_s]$ with $U_s = U_t \setminus \{u, v\}$. Extend π_s to an order π_t on G_t by keeping the same order on $V(G_s) = V(G_t)$ and adding the edge (u, v) . Since $v <_g u$, the edge (u, v) is backward with respect to π_t and is added to the matching. This yields a matching $M(\pi_t) = M(\pi_s) \cup \{(u, v)\}$, which is still a matching because $u, v \notin U_s$ and hence are unmatched in $M(\pi_s)$. The set of vertices in $W_t \setminus X_t$ and their unmatched status does not change when we add (u, v) , so the cost realised by π_t is exactly $c[s, g, U_t \setminus \{u, v\}]$. Thus the DP value in the second branch is achievable and does not underestimate the optimum.

(iii) Otherwise. There are two subcases:

- $v <_g u$ but at least one of u or v is not in U_t . Then in any feedback Morse order π extending g , the edge (u, v) is backward, so it must be included in $M(\pi)$ and both endpoints must be matched. This contradicts the requirement $U_t = V(M(\pi)) \cap X_t$, so the feasible set is empty and the correct value is $+\infty$.
- $v <_g u$ and $\{u, v\} \subseteq U_t$, but in the child graph one of u or v was already matched (equivalently, the child mask U_s would still contain that vertex). Then including the new backward edge (u, v) would match that vertex twice, violating the matching condition for $M(\pi)$. Thus no feedback Morse order is consistent with such a child state, and the correct value is again $+\infty$.

In either subcase, the recurrence correctly assigns $+\infty$.

Completeness.

Let π_t be any feedback Morse order on G_t consistent with (g, U_t) , and consider the status of the new edge (u, v) .

If $u <_g v$, then u precedes v in π_t , so (u, v) is forward and not in $M(\pi_t)$. Restricting π_t to G_s yields a feedback Morse order π_s whose restriction to $X_s = X_t$ is g and whose matched set on X_t is still U_t . The vertices in $W_s \setminus X_s$ are exactly those in $W_t \setminus X_t$, and their matched/unmatched status under π_s and π_t coincide. By the inductive hypothesis at s , the cost of π_s is at least $c[s, g, U_t]$, which equals the DP value $c[t, g, U_t]$ in this case.

If $v <_g u$, then v precedes u in π_t , so the new edge (u, v) is backward and must belong to $M(\pi_t)$; both u and v are matched, so $\{u, v\} \subseteq U_t$. Let $M_t := M(\pi_t)$ and restrict π_t and M_t to G_s , obtaining a feedback Morse order π_s on G_s with induced matching M_s . Since $(u, v) \notin E(G_s)$, the edge (u, v) is removed from the matching and no other matching edge in M_t is incident to u or v (by the matching property). Hence u and v are unmatched in M_s , and

$$V(M_s) \cap X_s = V(M_t) \cap X_t \setminus \{u, v\} = U_t \setminus \{u, v\}.$$

Thus π_s is consistent with the child state (g, U_s) , where $U_s = U_t \setminus \{u, v\}$. As in the forward case, $W_s \setminus X_s = W_t \setminus X_t$, and the unmatched vertices outside the bag are the same under π_s and π_t , with identical weights. By the inductive hypothesis at s , the cost of π_s is at least $c[s, g, U_t \setminus \{u, v\}]$, which is precisely the DP value $c[t, g, U_t]$ in this case.

In all cases, every feasible π_t has cost at least the DP value $c[t, g, U_t]$, so the DP does not overestimate the optimum. Together with soundness, this shows that the DP invariant holds at introduce-edge bags.

A.8 Forget-vertex bag

Let t be a forget-vertex bag with child s , forgetting vertex v . Then $X_t = X_s \setminus \{v\}$ and $G_t = G_s$. For each state (g, U_t) on X_t , where $g = (u_1, \dots, u_b)$ with $b = |X_t|$. For $i \in \{0, \dots, b\}$, let $\text{ins}_i(g, v)$ be the order on X_s obtained by inserting v between u_i and u_{i+1} , with sentinels u_0 and u_{b+1} before u_1 and after u_b .

By (T3), all edges incident to v have already been introduced below t , so the matching status of v is now final. Since $W_t = W_s$ and $X_t = X_s \setminus \{v\}$, we have

$$W_t \setminus X_t = (W_s \setminus X_s) \cup \{v\}.$$

The recurrence is:

$$c[t, g, U_t] = \min_{i=0, \dots, b} \min \left\{ c[s, \text{ins}_i(g, v), U_t] + \omega(v), \quad c[s, \text{ins}_i(g, v), U_t \cup \{v\}] \right\}.$$

Soundness.

Fix an insertion position i and consider the two child masks.

If we take the child state with order $\text{ins}_i(g, v)$ and mask U_t , we are asserting that v is *unmatched* in G_s under any feedback Morse order consistent with this state; that is, $v \notin V(M(\pi_s)) \cap X_s$. Since no further edges incident to v will appear above t by (T3), v will remain unmatched in any extension and must be counted in the objective exactly once, at the moment when it is forgotten. Adding $\omega(v)$ in this branch is therefore correct.

If instead we take the child state with mask $U_t \cup \{v\}$, we are asserting that v is already matched in G_s (to some vertex of G_s). Again by (T3), no new edges incident to v are introduced above t , so its matching status cannot change and v will never contribute to the unmatched-vertex cost at higher bags. Thus the second term correctly accounts for the case where v is matched.

Any child state that is not realisable by a feedback Morse order (for instance because v would be matched twice, or because it conflicts with already fixed backward edges) already carries value $+\infty$ by the inductive hypothesis, so it does not affect the minimum. Hence the recurrence does not underestimate the optimum.

Completeness.

Let π_t be any feedback Morse order on G_t consistent with (g, U_t) . Let i be such that in π_t the vertex v lies between u_i and u_{i+1} in the order on $X_s = X_t \cup \{v\}$; the restriction of π_t to X_s is then exactly $\text{ins}_i(g, v)$. There are two cases.

If v is unmatched in π_t , then $v \notin V(M(\pi_t))$, and since $U_t = V(M(\pi_t)) \cap X_t$, the child mask for X_s is

$$U_s = V(M(\pi_t)) \cap X_s = U_t.$$

Restricting π_t to G_s gives a feedback Morse order π_s on G_s consistent with the child state $(\text{ins}_i(g, v), U_t)$. The unmatched vertices in $W_s \setminus X_s$ under π_s are exactly those in $W_t \setminus X_t$

under π_t *excluding* v , and in addition v is unmatched and lies in $W_t \setminus X_t$. Thus the total unmatched weight under π_t is

$$(\text{unmatched weight in } W_s \setminus X_s) + \omega(v) \geq c[s, \text{ins}_i(g, v), U_t] + \omega(v),$$

by the inductive hypothesis at s .

If v is matched in π_t , then $v \in V(M(\pi_t))$, and

$$V(M(\pi_t)) \cap X_s = (V(M(\pi_t)) \cap X_t) \cup \{v\} = U_t \cup \{v\}.$$

Restricting π_t to G_s gives a feedback Morse order π_s on G_s consistent with the child state $(\text{ins}_i(g, v), U_t \cup \{v\})$. The unmatched vertices in $W_s \setminus X_s$ under π_s are exactly those in $W_t \setminus X_t$ under π_t , since $v \in X_s$ and is matched. By the inductive hypothesis at s , the total unmatched weight under π_s is at least

$$c[s, \text{ins}_i(g, v), U_t \cup \{v\}].$$

Taking the minimum over all insertion positions i and both cases matches the recurrence and shows that every feasible π_t has cost at least $c[t, g, U_t]$. Combined with soundness, the DP invariant holds at forget-vertex bags.

A.9 Join bag

Let t be a join bag with children s and s' , so that $X_t = X_s = X_{s'}$ and $G_t = G_s \cup G_{s'}$ with $V(G_s) \cap V(G_{s'}) = X_t$. By (T4), there are no edges of D between $W_s \setminus X_t$ and $W_{s'} \setminus X_t$, and hence no such edges in G_t . By (T5), every edge of D whose endpoints both lie in X_t is present in both G_s and $G_{s'}$.

Let (g, U_t) be an arbitrary state on X_t (i.e., a table entry). For this bag order g , the status of any edge with both endpoints in X_t is completely determined: such an edge (u, v) is backward (and therefore in the matching) if and only if it goes against g , i.e. if $v <_g u$; otherwise it is forward. We denote by $M_I(g) \subseteq X_t$ the set of vertices that are endpoints of bag-internal backward edges with respect to g . Any feedback Morse order π whose restriction to X_t is g must have $M_I(g) \subseteq V(M(\pi)) \cap X_t$.

At a join bag we combine states (g, U_s) from s and $(g, U_{s'})$ from s' such that:

- $M_I(g) \subseteq U_s, U_{s'}, U_t$, and
- outside $M_I(g)$, the sets of bag vertices matched strictly below t in the two subtrees are disjoint and their union equals the set of bag vertices matched strictly below t in the parent, i.e.

$$U_t \setminus M_I(g) = (U_s \setminus M_I(g)) \dot{\cup} (U_{s'} \setminus M_I(g)),$$

where $\dot{\cup}$ denotes disjoint union.

The recurrence is:

$$c[t, g, U_t] = \min_{\substack{U_s, U_{s'} \subseteq X_t \\ M_I(g) \subseteq U_s, U_{s'}, U_t \\ U_t \setminus M_I(g) = (U_s \setminus M_I(g)) \dot{\cup} (U_{s'} \setminus M_I(g))}} (c[s, g, U_s] + c[s', g, U_{s'}]),$$

and $c[t, g, U_t] = +\infty$ if no such pair $(U_s, U_{s'})$ exists.

Soundness.

Let $U_s, U_{s'}$ be masks satisfying the constraints above, and let π_s and $\pi_{s'}$ be feedback Morse orders on G_s and $G_{s'}$ consistent with (g, U_s) and $(g, U_{s'})$, respectively, and realising the DP values $c[s, g, U_s]$ and $c[s', g, U_{s'}]$.

We construct a feedback Morse order π_t on G_t as follows. For each interval between consecutive bag vertices in g (including before the first and after the last), collect:

- the vertices of $W_s \setminus X_t$ that appear in this interval in π_s , and
- the vertices of $W_{s'} \setminus X_t$ that appear in this interval in $\pi_{s'}$.

Within each side we preserve the relative order from π_s and $\pi_{s'}$. Then define π_t by listing:

- the bag vertices in the order g , and
- in each gap between consecutive bag vertices in g , first all vertices from $W_s \setminus X_t$ assigned to that gap, then all vertices from $W_{s'} \setminus X_t$ assigned to that gap, preserving their internal orders.

Because we preserve the relative order of vertices within each side and do not move any vertex across a bag vertex, the status (forward/backward) of every edge inside G_s or inside $G_{s'}$ is unchanged when passing from $\pi_s, \pi_{s'}$ to π_t . Edges with both endpoints in X_t are determined by g alone and have the same direction in all three orders. By (T4) there are no edges between $W_s \setminus X_t$ and $W_{s'} \setminus X_t$. Hence the set of backward edges in G_t with respect to π_t is exactly the union of the backward edges of π_s and $\pi_{s'}$, plus the bag-internal backward edges determined by g .

By the inductive hypothesis, the backward edges in G_s (resp. $G_{s'}$) form a matching, so within each side we have a matching. For bag-internal backward edges, the endpoints lie in $M_I(g)$, and by assumption each such vertex lies in both U_s and $U_{s'}$; these matches are the same in both subgraphs and thus represent a single set of matching edges on X_t . Outside $M_I(g)$, the sets of bag vertices matched strictly below t in the two subtrees are disjoint: this is enforced by the disjoint-union condition on U_s and $U_{s'}$. Together with the absence of edges between $W_s \setminus X_t$ and $W_{s'} \setminus X_t$, this implies that no vertex of G_t is incident to more than one matching edge, so the backward edges in G_t form a matching $M(\pi_t)$. Thus π_t is a feedback Morse order on G_t .

Moreover, the restriction of π_t to X_t is exactly g , and the vertices of X_t that are incident to backward edges in G_t are exactly those in U_t by the construction of the masks. No vertex is forgotten at t , and $W_s \setminus X_t$ and $W_{s'} \setminus X_t$ are disjoint, so the unmatched vertices in $W_t \setminus X_t$ are precisely the union of the unmatched vertices in $W_s \setminus X_t$ and $W_{s'} \setminus X_t$. Hence the total unmatched weight realised by π_t is

$$c[s, g, U_s] + c[s', g, U_{s'}],$$

and the DP value at t does not underestimate the optimum.

Completeness.

Conversely, let π_t be any feedback Morse order on G_t consistent with (g, U_t) . Restrict π_t to G_s and $G_{s'}$, obtaining feedback Morse orders π_s and $\pi_{s'}$. Let

$$U_s := V(M(\pi_s)) \cap X_t, \quad U_{s'} := V(M(\pi_{s'})) \cap X_t.$$

Bag-internal backward edges are determined by g and exist in all of G_s , $G_{s'}$, and G_t . Thus the set $M_I(g)$ of their endpoints is contained in $V(M(\pi_s)) \cap X_t$, in $V(M(\pi_{s'})) \cap X_t$, and in $V(M(\pi_t)) \cap X_t = U_t$; hence

$$M_I(g) \subseteq U_s, U_{s'}, U_t.$$

A vertex of X_t that is matched to a vertex in $W_s \setminus X_t$ cannot also be matched to a vertex in $W_{s'} \setminus X_t$, since $M(\pi_t)$ is a matching and there are no edges between $W_s \setminus X_t$ and $W_{s'} \setminus X_t$ by (T4). Therefore, outside $M_I(g)$, the sets U_s and $U_{s'}$ are disjoint, and their union is exactly the set of bag vertices matched strictly below t in π_t . Together with the fact that $M_I(g) \subseteq U_t$, this gives

$$U_t \setminus M_I(g) = (U_s \setminus M_I(g)) \dot{\cup} (U_{s'} \setminus M_I(g)),$$

so the pair $(U_s, U_{s'})$ is feasible for the join recurrence at t .

The unmatched vertices in $W_s \setminus X_t$ and in $W_{s'} \setminus X_t$ form a disjoint union equal to the set of unmatched vertices in $W_t \setminus X_t$, so the total unmatched weight of π_t is

$$(\text{unmatched weight in } W_s \setminus X_t) + (\text{unmatched weight in } W_{s'} \setminus X_t) \geq c[s, g, U_s] + c[s', g, U_{s'}],$$

by the inductive hypothesis applied at s and s' . Taking the minimum over all feasible pairs $(U_s, U_{s'})$ in the recurrence gives that the DP value $c[t, g, U_t]$ at t is at most this cost. Thus every feasible π_t has cost at least $c[t, g, U_t]$, so the DP does not overestimate either.

Hence the DP invariant holds at join bags.

A.10 Global correctness

By induction on the tree decomposition, the DP invariant holds at every bag. At the root bag r we have $X_r = \emptyset$, so there is a single state (\emptyset, \emptyset) , whose value $c[r, \emptyset, \emptyset]$ is, by the invariant, the minimum total weight of unmatched vertices over all feedback Morse orders on the entire digraph D . By Corollary 18, this is exactly the optimum value of FMM on D . This proves the correctness of the algorithm.

A.11 Running time analysis

We now bound the running time of the dynamic program in terms of the treewidth k of the underlying undirected graph of D and the number of vertices $n := |V(D)|$. Throughout, we work with a nice tree decomposition of width k and $O(n)$ bags, refined with introduce-edge bags.

Number of states per bag.

Let t be a bag with vertex set X_t and $b := |X_t| \leq k + 1$. A DP state at t consists of:

- a total order g on X_t , and
- a subset $U \subseteq X_t$ indicating which bag vertices are already matched (to other vertices either in X_t or strictly below t).

There are $b!$ possible orders and 2^b possible subsets, so the number of states at t is at most

$$N_t \leq b! \cdot 2^b \leq (k + 1)! \cdot 2^{k+1}.$$

Using Stirling's approximation, $(k + 1)! = 2^{\Theta(k \log k)}$, so $N_t = 2^{O(k \log k)}$. Since the nice tree decomposition has $O(n)$ bags, the total table size over all bags is $2^{O(k \log k)} \cdot n$.

Cost per bag.

We now argue that at each bag the work per state is bounded by $2^{O(k)}$, so the factorial term $(k + 1)!$ dominates and the total running time is $2^{O(k \log k)} \cdot n$.

Leaf and introduce-vertex bags. At a leaf bag there is a single state with constant-time initialisation.

At an introduce-vertex bag t with child s , we have $X_t = X_s \cup \{v\}$. For each state (g', U_t) on X_t we:

- check whether $v \in U_t$, and
- if not, map (g', U_t) to the unique child state (g, U_s) with g the restriction of g' to X_s and $U_s = U_t \cap X_s$.

This can be done in time polynomial in b (e.g. $O(b)$) per state, so the total cost at t is $O(N_t \cdot b) = 2^{O(k \log k)}$.

Introduce-edge bags. At an introduce-edge bag t with child s , introducing an edge (u, v) , we have $X_t = X_s$. For each state (g, U_t) on X_t the recurrence examines the relative order of u and v in g and the membership of u and v in U_t , and possibly maps to a single child state (g, U_s) or concludes that the state is infeasible. All of this is constant-time work per state. Thus the total cost at t is $O(N_t) = 2^{O(k \log k)}$.

Forget-vertex bags. At a forget-vertex bag t with child s , forgetting v , we have $X_t = X_s \setminus \{v\}$ and $b = |X_t|$. For each state (g, U_t) on X_t we consider all $b+1$ possible insertion positions of v into the order g , and for each position i we look up at most two child states:

$$(\text{ins}_i(g, v), U_t) \quad \text{and} \quad (\text{ins}_i(g, v), U_t \cup \{v\}).$$

Thus the cost per parent state is $O(b)$ table accesses and $O(b)$ simple operations, and the total cost at t is

$$O(N_t \cdot b) = 2^{O(k \log k)}.$$

Join bags. At a join bag t with children s and s' , we have $X_t = X_s = X_{s'}$ and $G_t = G_s \cup G_{s'}$ with $V(G_s) \cap V(G_{s'}) = X_t$. The order component g is the same in all three bags, so we process each order g independently.

Fix an order g on X_t . The bag-internal backward edges with respect to g and the corresponding set of endpoints $M_I(g)$ can be computed in time $O(b^2)$ once per g . For this fixed g , we now combine masks: for each parent mask $U_t \subseteq X_t$ we consider those child masks $U_s, U_{s'} \subseteq X_t$ that satisfy the constraints in the join recurrence, i.e.

$$M_I(g) \subseteq U_s, U_{s'}, U_t, \quad \text{and} \quad U_t \setminus M_I(g) = (U_s \setminus M_I(g)) \dot{\cup} (U_{s'} \setminus M_I(g)).$$

Equivalently, for each $x \in X_t \setminus M_I(g)$:

- if $x \in U_t$, it must be in exactly one of U_s or $U_{s'}$;
- if $x \notin U_t$, it must be in neither U_s nor $U_{s'}$.

Thus for fixed (g, U_t) there are at most $2^{|U_t \setminus M_I(g)|} \leq 2^b$ valid pairs $(U_s, U_{s'})$, and we simply take the minimum of $c[s, g, U_s] + c[s', g, U_{s'}]$ over those pairs. The work per parent state is therefore $O(2^b)$ table accesses, and the total cost at t is

$$O(N_t \cdot 2^b) \leq (b! \cdot 2^b) \cdot 2^b = b! \cdot 2^{2b} = 2^{O(k \log k)}.$$

Global bound.

Each of the $O(n)$ bags performs $2^{O(k \log k)}$ work, dominated by the factorial number of orders on a bag. Summing over all bags, the total running time is

$$2^{O(k \log k)} \cdot n.$$

This establishes the running-time bound claimed in the theorem: the FEEDBACK MORSE ORDER problem (and hence FMM) is fixed-parameter tractable when parameterized by the treewidth k of the underlying undirected graph of the digraph D .

B WiPS-reduction Details

We require the following lemma and proposition to hold for the spaces constructed during the reduction. They are direct consequences of the structural properties of the gadgets used in the construction.

► **Lemma 19.** *Every optimal solution to the ERASIBILITY problem can be chosen to contain only detonator simplices.*

► **Proposition 20.** *Let S be a set of 2-simplices whose deletion makes certain subcomplexes erasible. Then:*

1. *If the detonator of a gadget becomes erasible, then all its outgoing locks are erasible.*
2. *If every incoming lock of a fuse is erasible, then the entire fuse is erasible.*
3. *If all outgoing locks are erasible while some incoming lock is not, then S contains at least one simplex from the gadget itself.*

The proofs of Lemma 19 and Proposition 20 rely on the properties outlined below and follow directly from them.

B.1 Induction Hypothesis

We perform a structural induction over a nice tree decomposition $TD(D)$ of width k for the digraph D to construct a simplicial complex Y . More precisely, we define complexes Y_t for each bag X_t of $TD(D)$; the final space Y is the complex Y_r associated with the root bag X_r . Simultaneously we construct a tree decomposition of the Hasse diagram of Y_t , denoted $TD(Y_t)$, of width at most $c \cdot k$ for a fixed constant c . Our goal is to prove that Y is erasible after removing at most s simplices if and only if D has a feedback vertex set of size s . To achieve this we require the following induction hypothesis, divided into three groups of conditions.

► **Definition 21 (Aglet).** *Let K be a 2-dimensional simplicial complex and let A be a subset of its 1-simplices. We say that K is erasible modulo the aglet A if there exists a sequence of elementary collapses of K in which no collapse involves an edge from A . The term aglet—meaning the small tip at the end of a shoelace that prevents fraying—is chosen because in our constructions the complex can only “unravel” from these edges: if the aglet edges cannot be collapsed, the entire structure remains intact.*

Conditions on the subcomplexes composing Y_t :

- Y_t is the union of nonempty subcomplexes Y_t^v , one for each vertex $v \in F_t \cup X_t$.
- Each Y_t^v is the union of two subcomplexes: the locks $\mathcal{L}(v)$ and the fuse $\mathcal{F}(v)$.
- The family $\{\mathcal{L}(v), \mathcal{F}(v) \mid v \in F_t \cup X_t\}$ partitions the set of 2-simplices in Y_t .
- For each v , both $\mathcal{L}(v)$ and $\mathcal{F}(v)$ contain a distinguished boundary component, denoted $\mathcal{L}_B(v)$ and $\mathcal{F}_B(v)$ respectively.
- If $v \in X_t$ then $\mathcal{L}_B(v) \cap \mathcal{F}_B(v) = \emptyset$; if $v \in F_t$ then $\mathcal{L}_B(v) = \mathcal{F}_B(v)$.

Conditions on the tree decomposition $TD(Y_t)$ of Y_t :

- $TD(Y_t)$ is a valid tree decomposition of the Hasse diagram of Y_t .

- $TD(Y_t)$ includes a distinguished bag $R_t = \bigsqcup_{v \in X_t} (\mathcal{L}_B(v) \sqcup \mathcal{F}_B(v))$, which serves as the interface to the parent bag.
- The width of $TD(Y_t)$ is at most $c \cdot k$ for a fixed constant c .

Crucial properties of Y_t :

1. For every vertex $u \in X_t \cup F_t$, the subcomplex $\mathcal{L}(u)$ is a connected manifold and becomes erasible if any 2-simplex is deleted from it;
2. If $v \in X_t \cup F_t$ and all $\mathcal{L}(u)$ with an edge uv from a forgotten vertex $u \in F_t$ to v are erasible, then $\mathcal{F}(v)$ is erasible;
3. If $u \in F_t$ and $\mathcal{F}(u)$ is erasible, then $\mathcal{L}(u)$ is erasible as well;
4. If $u \in X_t$, then the only free faces of $\mathcal{L}(u)$ lie on $\mathcal{L}_B(u)$;
5. If uv is an edge with at least one endpoint in F_t , then there is a cylindrical subcomplex $Cyl_t(u, v) \subseteq \mathcal{F}(v)$ whose two boundary components are attached respectively to a handle of $\mathcal{L}(u)$ and to the boundary $\mathcal{F}_B(v)$ of the fuse.

B.2 Notation

We prove by structural induction over the nice tree decomposition $TD(D)$ that the spaces Y_t constructed at each bag X_t satisfy the induction hypothesis. The construction for each bag type is illustrated in Figures 17–20. In every step, verification proceeds directly by inspection of the figure and the local structure of the gadgets.

B.3 Leaf bag.

Let t be the (unique) empty leaf of the nice tree decomposition, so $X_t = \emptyset$, and set $Y_t = \emptyset$. There are no vertices in $F_t \cup X_t$, hence there are no subcomplexes Y_t^v , no lock or fuse parts, and no distinguished boundary components; all structural clauses of the induction hypothesis hold trivially.

The Hasse diagram of Y_t is empty, so $TD(Y_t)$ consists of a single empty bag. We designate this unique bag as the interface bag

$$R_t = \bigsqcup_{v \in X_t} (\mathcal{L}_B(v) \sqcup \mathcal{F}_B(v)) = \emptyset.$$

By the usual convention tw of the empty graph is -1 , hence $\text{tw}(TD(Y_t)) \leq ck$. Finally, since there are no vertices or edges, each of the crucial properties (1)–(5) holds vacuously.

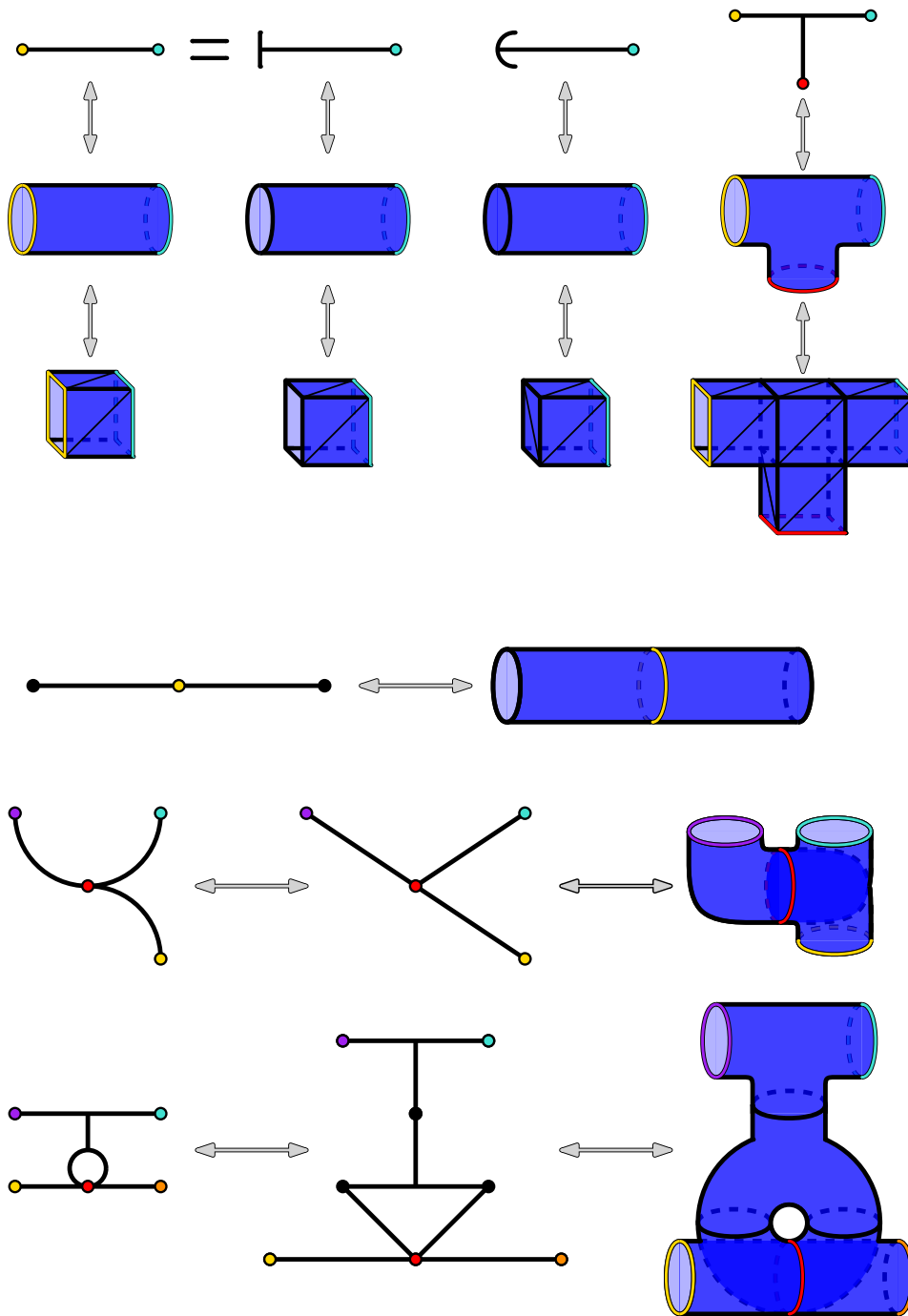
B.4 Introduce vertex.

Let t be an introduce-vertex node with child t' and $X_t = X_{t'} \cup \{v\}$. From the complex $Y_{t'}$, we construct Y_t by (i) attaching a fresh gadget Y_t^v for the new vertex v , and (ii) extending each existing aglet boundary by a short collar cylinder so that the global aglet remains the disjoint union of the designated boundary components.

New gadget. The gadget Y_t^v consists of two disjoint components,

$$Y_t^v = \mathcal{F}(v) \sqcup \mathcal{L}(v).$$

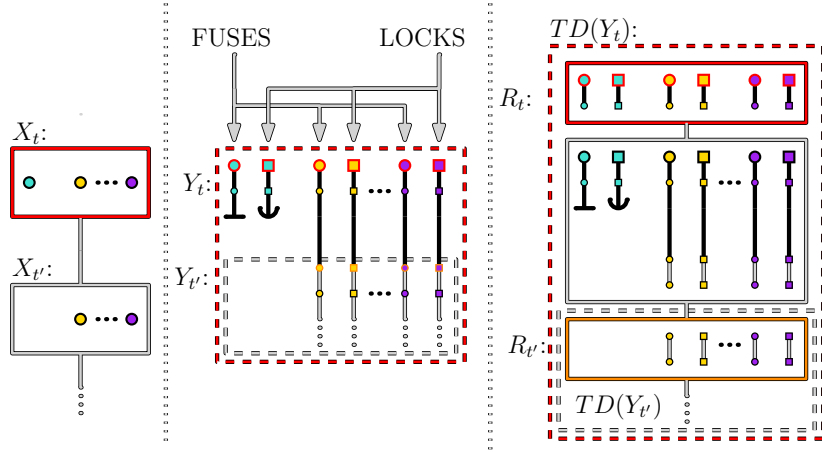
The *fuse* $\mathcal{F}(v)$ is a cylinder whose one boundary circle, denoted $\mathcal{F}_B(v)$, is attached to the current aglet boundary of $Y_{t'}$; its opposite boundary is left free and becomes part of the new aglet. The *lock* $\mathcal{L}(v)$ is a cylinder capped by a disc, with open boundary circle $\mathcal{L}_B(v)$ attached along the aglet. The two components are disjoint at this step, satisfying $\mathcal{F}_B(v) \cap \mathcal{L}_B(v) = \emptyset$.



■ **Figure 16** Elementary and composite gadget components used in the construction. Tubes, pairs of pants, and locks (cylinders with handles) serve as the basic building blocks for the fuse and lock regions.

Geometrically, $\mathcal{F}(v)$ is erasible *modulo* $\mathcal{F}_B(v)$ by collapsing from its free end, whereas $\mathcal{L}(v)$ is not erasible *modulo* $\mathcal{L}_B(v)$ since all its free faces lie on the aglet.

Extending existing components. For every $u \in X_{t'} \cup F_{t'}$, we glue a collar cylinder along each



■ **Figure 17** Inductive construction of Y_t for an introduce-vertex bag. Left: fragment of the nice tree decomposition, where t' is the child of t and v is introduced. Middle: attaching the new gadget $Y_t^v = \mathcal{F}(v) \sqcup \mathcal{L}(v)$ and collaring existing aglet boundaries. Right: the corresponding update of the tree decomposition $TD(Y_t)$ with the interface bag R_t containing all aglet circles for X_t .

boundary component in $\mathcal{F}_B(u)$ or $\mathcal{L}_B(u)$ and redefine the aglet to be the outer boundary of the collar. This operation is a product extension that preserves all local incidences and does not alter erasibility *modulo the aglet*.

In particular, all structural and erasibility properties of the subcomplexes $Y_{t'}^u$ remain unchanged.

Verification of the induction hypothesis. The new complex Y_t satisfies every clause of the induction hypothesis:

- *Composition:* Y_t is the union of nonempty subcomplexes Y_t^w for $w \in X_t \cup F_t$, each decomposed as $\mathcal{F}(w) \cup \mathcal{L}(w)$. The family $\{\mathcal{F}(w), \mathcal{L}(w)\}$ partitions the set of 2-simplices. For all $w \in X_t$, $\mathcal{F}_B(w) \cap \mathcal{L}_B(w) = \emptyset$, and for $w \in F_t$ the equality $\mathcal{F}_B(w) = \mathcal{L}_B(w)$ remains valid.
- *Tree decomposition:* Starting from $TD(Y_{t'})$ with distinguished bag $R_{t'}$, we add $O(\deg(v))$ new bags of constant size covering the simplices of Y_t^v and the collars, each attached adjacent to $R_{t'}$. The new interface bag is

$$R_t = \bigsqcup_{w \in X_t} (\mathcal{L}_B(w) \sqcup \mathcal{F}_B(w)),$$

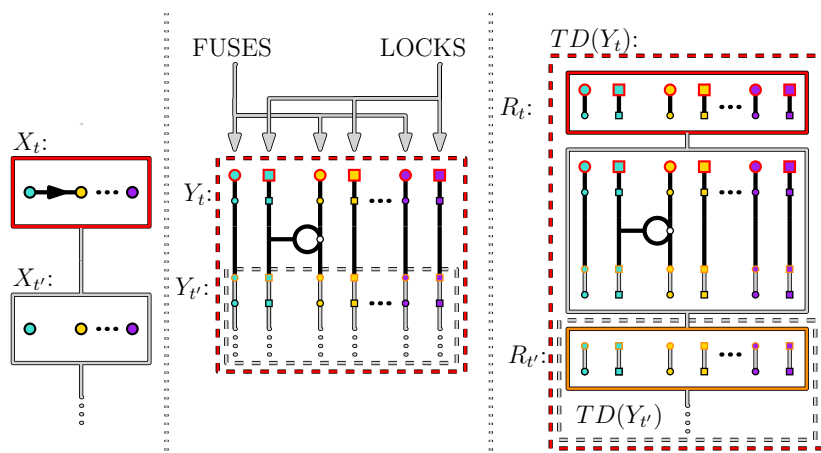
which includes all current aglet edges. The running-intersection property is preserved, and the width increases by at most a fixed constant c_1 , so $\text{tw}(TD(Y_t)) \leq c \cdot k$.

- *Crucial properties:* (1) Each $\mathcal{L}(u)$ remains a connected manifold erasible after deletion of any 2-simplex. (2) No new incoming attachments are created for v , so the property for fuses is unchanged. (3) For forgotten vertices $u \in F_t$, the implication “ $\mathcal{F}(u)$ erasible $\Rightarrow \mathcal{L}(u)$ erasible” still holds. (4) For $u \in X_t$, the only free faces of $\mathcal{L}(u)$ lie on $\mathcal{L}_B(u)$. (5) No new edge cylinders $Cyl_t(u, v)$ are introduced at this step; those from $Y_{t'}$ persist unchanged up to the collars.

Hence all parts of the induction hypothesis are preserved, and the width of the tree decomposition increases by at most a constant in the introduce-vertex step.

B.5 Introduce edge.

Let X_t be an introduce-edge bag that adds the directed arc (u, v) with $u, v \in X_t$. From $Y_{t'}$ we first extend every aglet boundary by a short *collar* (a thin cylinder), ensuring that all new attachments are placed away from the current aglet circles.¹ We then realize the edge (u, v) by an *edge handle* that couples the lock of u to the fuse of v (cf. Figure 18):



■ **Figure 18** Inductive construction of Y_t for an introduce-edge bag that adds the arc (u, v) with $u, v \in X_t$. Left: fragment of the tree decomposition with child t' and bag X_t containing both endpoints. Middle: collaring the aglets and attaching a lock-side stub to $\mathcal{L}(u)$ together with the cylindrical band $Cyl_t(u, v) \subseteq \mathcal{F}(v)$. Right: the local update of $TD(Y_t)$ by a small number of bags covering the new simplices and keeping R_t as the aglet interface.

1. **Lock-side stub.** A short 1-handle stub is attached to $\mathcal{L}(u)$ along a circle parallel to $\mathcal{L}_B(u)$. This stub is part of $\mathcal{L}(u)$ and meets the complex only along its attaching circle. It introduces no new free faces except on $\mathcal{L}_B(u)$.
2. **Fuse-side clasp.** Attach a thin cylindrical band

$$Cyl_t(u, v) \subseteq \mathcal{F}(v),$$

whose two boundary circles glue respectively (i) to the terminal circle of the lock-side stub from (1) and (ii) to the collar of $\mathcal{F}(v)$ near $\mathcal{F}_B(v)$. All 2-simplices of this band belong to $\mathcal{F}(v)$.

Intuitively, the handle-clasp blocks any collapse of $\mathcal{F}(v)$ from its aglet side while the handle remains attached. Once $\mathcal{L}(u)$ becomes erasible (for instance after its incoming locks are erased or its detonator is deleted), the lock-side stub collapses and the clasp detaches, restoring erasibility of $\mathcal{F}(v)$. No new free faces are created away from aglet boundaries.

Preservation of the induction hypothesis.

- *Subcomplex partition and interfaces.* Every new 2-simplex is assigned to exactly one gadget: the stub to $\mathcal{L}(u)$ and the band $Cyl_t(u, v)$ to $\mathcal{F}(v)$. Distinct boundary components remain valid: for all $w \in X_t$, $\mathcal{L}_B(w) \cap \mathcal{F}_B(w) = \emptyset$; for all $w \in F_t$, $\mathcal{L}_B(w) = \mathcal{F}_B(w)$.

¹ Collars serve as safe neighborhoods: they separate old and new attachments and guarantee that no unintended free faces appear when handles are glued.

- *Crucial properties (1)–(5).* Property (5) is realized by $Cyl_t(u, v)$: one boundary circle attaches to a handle of $\mathcal{L}(u)$, the other to $\mathcal{F}_B(v)$. Properties (1), (3), and (4) still hold because the stub lies entirely in $\mathcal{L}(u)$ and introduces no free faces except on $\mathcal{L}_B(u)$. Property (2) follows from the clasp mechanism: $\mathcal{F}(v)$ cannot begin collapsing at its aglet while any incoming lock remains uncollapsed; once all incoming locks $\mathcal{L}(\cdot)$ attached to v are erasible, $\mathcal{F}(v)$ itself becomes erasible.

Tree decomposition update. Extend $TD(Y_{t'})$ by two new bags:

- a bag B_t^{edge} that contains all Hasse nodes of the new simplices introduced at step t (collars, lock-side stub, and the band $Cyl_t(u, v)$), together with the incident aglet edges they meet; and
- a bag B_t^{collar} containing only the collar cylinders (their 2-simplices, boundary 1-simplices, and adjacent 0-simplices), ensuring connectivity and running-intersection for the boundary nodes.

Attach B_t^{edge} to a bag of $TD(Y_{t'})$ that already contains the aglet circles of $\mathcal{L}_B(u)$ and $\mathcal{F}_B(v)$, and make B_t^{collar} adjacent to B_t^{edge} . Update the distinguished interface bag to

$$R_t := \bigsqcup_{w \in X_t} (\mathcal{L}_B(w) \sqcup \mathcal{F}_B(w)),$$

taking each boundary circle on the *outer* end of its new collar. Only $O(1)$ simplices and incidences are introduced per edge, so the width of the decomposition increases by at most a constant factor independent of k .

Remarks. The step fully preserves the inductive invariants, provided that:

- each clasp circle on the fuse side is not a free 1-simplex after attachment;
- the lock-stub seam remains non-free within $\mathcal{L}(u)$; and
- every incoming edge to v contributes exactly one clasp covering the corresponding boundary of $\mathcal{F}(v)$.

These are straightforward geometric checks in the explicit triangulation and hold for the gadgets shown in the construction figures.

B.6 Join.

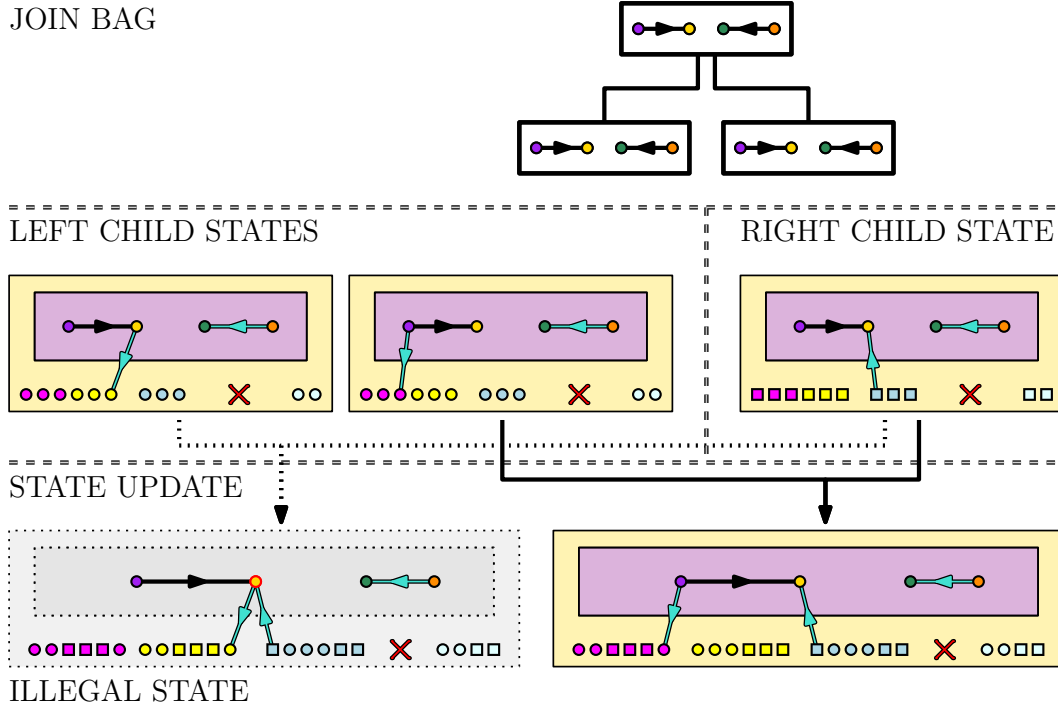
Let t be a join node with children t_1, t_2 and $X_{t_1} = X_{t_2} = X_t$. We obtain Y_t from Y_{t_1} and Y_{t_2} by synchronizing, for each $v \in X_t$, the fuse and lock interfaces as follows (see Figure 19).

Fuses. Introduce a new cylinder $Cyl^{\text{join}}(v)$ and glue both child fuse aglets $\mathcal{F}_B^{t_1}(v)$ and $\mathcal{F}_B^{t_2}(v)$ to one boundary circle of $Cyl^{\text{join}}(v)$. The other boundary circle becomes the new fuse aglet $\mathcal{F}_B(v)$ in Y_t . This enforces that $\mathcal{F}(v)$ in Y_t is erasible only if both child fuses were erasible; conversely, if both child fuses erase then $Cyl^{\text{join}}(v)$ collapses to expose $\mathcal{F}_B(v)$ as required.

Locks. Introduce a pair-of-pants surface $P^{\text{join}}(v)$, glue its two legs to the child lock aglets $\mathcal{L}_B^{t_1}(v)$ and $\mathcal{L}_B^{t_2}(v)$, and designate the waist as the new lock aglet $\mathcal{L}_B(v)$. If $\mathcal{L}_B(v)$ becomes free, then $P^{\text{join}}(v)$ collapses and, in turn, both child lock components erase; if either child lock is erasible, the connection makes the other erasible as well. No free faces are created away from aglet circles, so properties about free faces remain localized to aglets.

Preservation of the induction hypothesis. After the two gluings for each $v \in X_t$, the partition $Y_t = \bigsqcup_{v \in X_t \cup F_t} Y_t^v$ is maintained, and within each Y_t^v the sets of 2-simplices still partition into $\mathcal{L}(v) \sqcup \mathcal{F}(v)$. Each $\mathcal{L}(v)$ and $\mathcal{F}(v)$ remains connected, and their new aglets $\mathcal{L}_B(v)$ and $\mathcal{F}_B(v)$ are disjoint. Clause (2) (fuse erasibility from incoming locks) is preserved because the fuse-side synchronization is conjunctive, while clause (3) (locks follow erasible fuses for

JOIN BAG



■ **Figure 19** Inductive construction of Y_t for a join bag with children t_1, t_2 and $X_{t_1} = X_{t_2} = X_t$. Left: the two subtrees rooted at t_1 and t_2 joining at t . Middle: synchronization of gadgets for each $v \in X_t$ by joining the child fuse aglets via a cylinder $Cyl^{join}(v)$ and the child lock aglets via a pair-of-pants $P^{join}(v)$. Right: the update of $TD(Y_t)$ using a linking bag for the new simplices and a collar bag whose vertex set is the new aglet interface R_t .

forgotten vertices) and clause (4) (free faces only at aglets for active vertices) continue to hold by locality of the attachments. The edge handles $Cyl(u, v)$ that attach to $\mathcal{L}_B(\cdot)$ or $\mathcal{F}_B(\cdot)$ continue to attach to the new aglets, so clause (5) (existence and placement of cylinders) is preserved.

Tree decomposition update. Let R_{t_1} and R_{t_2} denote the designated top bags of the children. We add a new *linking bag* B_t^{link} that contains: (i) all newly created simplices (the cylinders $Cyl^{join}(v)$ and pairs-of-pants $P^{join}(v)$ together with their incident boundaries), and (ii) the child collar circles, i.e., the aglet boundaries $\{\mathcal{F}_B^{t_i}(v), \mathcal{L}_B^{t_i}(v) \mid v \in X_t, i \in \{1, 2\}\}$. We make R_{t_1} and R_{t_2} the children of B_t^{link} . On top of B_t^{link} we add a *collar bag* B_t^{collar} that contains precisely the new aglet circles

$$R_t := \bigsqcup_{v \in X_t} (\mathcal{L}_B(v) \sqcup \mathcal{F}_B(v)),$$

and we declare R_t to be the designated interface bag of Y_t . All additions are of constant size per vertex in X_t , so the width increases by at most a fixed constant, preserving the $O(k)$ bound.

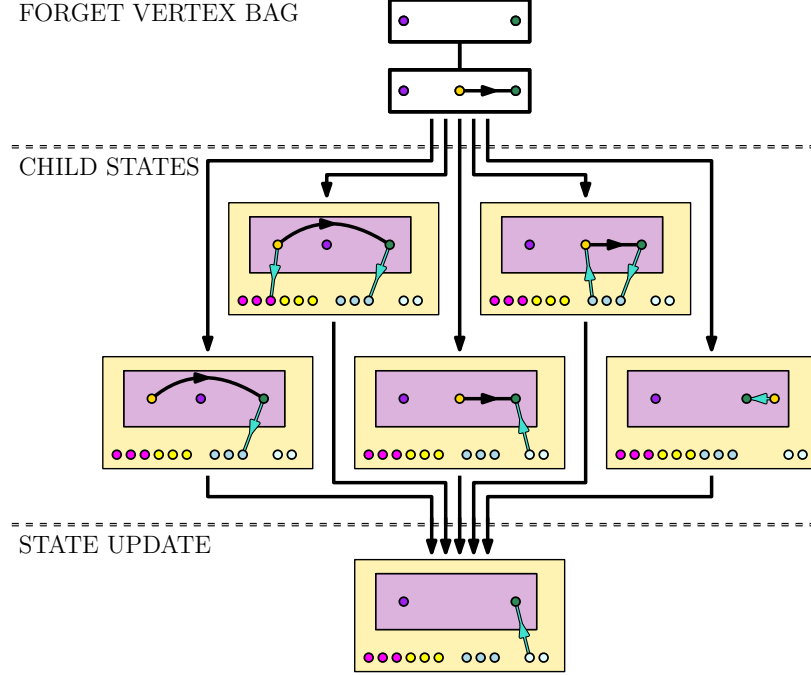
B.7 Forget vertex.

Let $u \in X_{t'}$ be the vertex forgotten at t , and write $Y_{t'} = Y_{t'}^u \cup \bigcup_{v \in X_{t'} \setminus \{u\}} Y_{t'}^v$ with $Y_{t'}^u = \mathcal{F}(u) \cup \mathcal{L}(u)$. At the forget step we *identify the aglets* of u by gluing the boundary

circles

$$\mathcal{F}_B(u) \equiv \mathcal{L}_B(u)$$

simplicially, possibly after a constant-size refinement of the two circles so that their triangulations agree.



■ **Figure 20** Inductive construction of Y_t for a forget-vertex bag that forgets u . Left: fragment of the tree decomposition with child t' and $X_t = X_{t'} \setminus \{u\}$. Middle: identifying the aglets $\mathcal{F}_B(u)$ and $\mathcal{L}_B(u)$ into a single boundary circle and collaring the remaining aglets for vertices in X_t . Right: the corresponding update of $TD(Y_{t'})$, where u disappears from the interface bag $R_{t'}$ and only aglet circles for X_t remain.

After this identification Y_t is obtained from $Y_{t'}$ by: (i) unifying $\mathcal{F}_B(u)$ and $\mathcal{L}_B(u)$ into a single boundary cycle, (ii) leaving all incident edge-handles $Cyl_{t'}(w, u) \subseteq \mathcal{F}(u)$ and attachments from $\mathcal{L}(u)$ untouched (they remain attached exactly as before), and (iii) extending every remaining aglet $\mathcal{F}_B(v)$ and $\mathcal{L}_B(v)$ for $v \in X_{t'} \setminus \{u\}$ by a collar cylinder (which merely moves each aglet outward).

Verification of the induction hypothesis. We check each block of clauses.

(Subcomplex structure). The family $\{Y_t^v\}_{v \in F_t \cup X_t}$ is obtained from $\{Y_{t'}^v\}$ by removing u from $X_{t'}$ and placing it into F_t . For every $v \in F_t \cup X_t$, Y_t^v still splits as $\mathcal{L}(v) \cup \mathcal{F}(v)$, and the 2-simplices of Y_t are still partitioned by $\{\mathcal{L}(v), \mathcal{F}(v)\}$. For $v \in X_t$ the distinguished boundaries $\mathcal{L}_B(v)$ and $\mathcal{F}_B(v)$ remain disjoint; for $v \in F_t$ they coincide. For the forgotten u , by construction $\mathcal{L}_B(u) = \mathcal{F}_B(u)$, as required.

(Tree decomposition). From $TD(Y_{t'})$ we create two bags:

$$B_t^{\text{forget}} \supset R_{t'} \cup (\mathcal{F}_B(u) \cup \mathcal{L}_B(u)) \cup (\text{all 1- and 2-simplices incident to these circles}),$$

and a collar bag B_t^{collar} containing only the collar cylinders attached at this step. We then

set

$$R_t := \bigsqcup_{v \in X_t} (\mathcal{L}_B(v) \sqcup \mathcal{F}_B(v)),$$

so u no longer contributes to the interface. Each new bag consists of a constant number of constant-size pieces per $v \in X_t$, hence $\text{width}(TD(Y_t)) \leq c \cdot \text{width}(TD(Y_{t'})) + c_0 = O(k)$.

(*Crucial properties*). (1) $\mathcal{L}(u)$ remains a connected manifold; if any 2-simplex of $\mathcal{L}(u)$ is deleted then $\mathcal{L}(u)$ collapses completely (unchanged by the boundary identification). (2) For any v , incoming locks from forgotten vertices behave as before; the identification at u does not create new incoming constraints for other vertices, and the collar extensions merely relocate aglets, preserving erasibility modulo aglets. (3) If $\mathcal{F}(u)$ is erasible then, after collapsing $\mathcal{F}(u)$, the identified circle becomes a degree-one edge in $\mathcal{L}(u)$, so $\mathcal{L}(u)$ collapses entirely. (4) For every $x \in X_t$, no new free faces appear in $\mathcal{L}(x)$ except on $\mathcal{L}_B(x)$; the forget operation affects only u 's boundary and does not introduce side faces elsewhere. (5) For every edge with at least one endpoint in F_t , the cylindrical subcomplex $\text{Cyl}_t(\cdot, \cdot)$ already present in $\mathcal{F}(\cdot)$ is preserved; handles attached to $\mathcal{L}(u)$ and cylinders ending on $\mathcal{F}_B(u)$ remain attached to the unified Y_t^u exactly as before the identification.

Effect on erasibility. Gluing $\mathcal{F}_B(u)$ to $\mathcal{L}_B(u)$ enforces that once all incoming locks to u have been released so that $\mathcal{F}(u)$ collapses, the shared aglet becomes a free edge of $\mathcal{L}(u)$, and then $\mathcal{L}(u)$ collapses as well. Conversely, deleting any 2-simplex of $\mathcal{L}(u)$ makes $\mathcal{L}(u)$ erasible; after its removal, the shared boundary is exposed on the fuse side and does not create new obstructions for other gadgets. Collar extensions do not change these implications; they only move aglets outward.

B.8 Width bound.

At each inductive step, the modification of the complex is strictly local and affects only a constant number of simplices per vertex in the active bag. Specifically:

- In an *introduce vertex* step, we add a single fuse–lock gadget of constant size;
- In an *introduce edge* step, we add one constant-size handle connecting existing boundary components;
- In a *forget vertex* step, we glue together two constant-size boundary components;
- In a *join* step, we attach one cylinder and one pair-of-pants per vertex in the shared bag.

In each case, the corresponding update of the tree decomposition introduces at most two additional bags (a *linking bag* containing the new simplices and a *collar bag* containing the updated boundary circles). Each bag therefore contains at most $O(|X_t|)$ elements, with a constant factor determined solely by the size of the gadgets. Hence, if the treewidth of $TD(D)$ is k , then the treewidth of the Hasse diagram of the constructed complex satisfies

$$\text{tw}(TD(Y_t)) \leq c \cdot k + c_0$$

for fixed constants c, c_0 independent of D . This establishes the width-preserving property required by the Width Preserving Strategy (WiPS).

B.9 Conclusion.

By direct verification for each bag type—introduce vertex, introduce edge, forget vertex, and join—the structural and erasibility properties listed in the induction hypothesis remain valid after each construction step. In particular:

- every Y_t decomposes into vertex gadgets $\{Y_t^v\}$ satisfying the fuse–lock partitioning;
- all topological and erasibility properties (Items 1–5 of the hypothesis) are preserved by the local gluings; and
- the width bound established above holds uniformly across all steps.

Therefore, at the root bag r the resulting space $Y = Y_r$ satisfies all clauses of the induction hypothesis and has Hasse diagram treewidth $O(k)$. This completes the inductive construction of a low-treewidth simplicial complex corresponding to the digraph D .

B.10 Correctness

Finally, we get to the proof that the above construction actually gives a parameterized reduction from the FVS problem to the Erasibility problem. We do this by showing that the graph D has a feedback vertex set S of size s if and only if we can remove a set S' of simplices so that the space Y_r is erasible. The forward direction is Proposition 22 and the backwards direction is Proposition 23.

► **Proposition 22.** *If S is a feedback vertex set in D , then $Y_r \setminus S'$ is erasible, where*

$$S' = \{\text{detonator}(u) \mid u \in S\}.$$

Proof. By the completed construction, Y_r satisfies the structural clauses and the “Crucial properties (1)–(5)” from the Induction Hypothesis, and the gadget implications in Proposition 20.

Since S is a feedback vertex set, $D \setminus S$ is acyclic. Fix a topological ordering v_1, \dots, v_m of $V \setminus S$ (so every arc (v_i, v_j) in $D \setminus S$ has $i < j$).

Step 1 (delete detonators; collapse \mathcal{L} for S). Remove S' from Y_r . For each $u \in S$, the detonator lies in $\mathcal{L}(u)$; by Crucial Property (1), deleting any 2-simplex in $\mathcal{L}(u)$ makes $\mathcal{L}(u)$ erasible. Collapse every $\mathcal{L}(u)$ completely. All attachments along these locks are thus released.

Step 2 (erase gadgets along the topological order of $D \setminus S$). We claim that for $j = 1, \dots, m$ the gadget $Y_r^{v_j} = \mathcal{F}(v_j) \cup \mathcal{L}(v_j)$ can be erased.

Fix j . Every incoming arc $u \rightarrow v_j$ has $u \in S$ or $u = v_i$ with $i < j$. In either case, the corresponding lock $\mathcal{L}(u)$ is already erasible (it was collapsed in Step 1 if $u \in S$, or it was collapsed when $Y_r^{v_i}$ was removed earlier). Hence all incoming locks of v_j are erasible. By Proposition 20(2) the fuse $\mathcal{F}(v_j)$ is erasible; after collapsing $\mathcal{F}(v_j)$, Crucial Property (3) implies $\mathcal{L}(v_j)$ is erasible. Thus $Y_r^{v_j}$ erases completely.

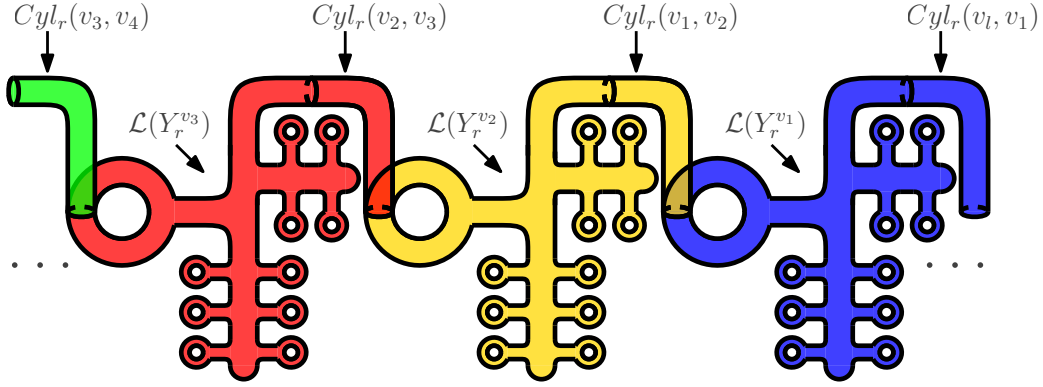
Step 3 (cleanup for S). After all v_1, \dots, v_m have been erased, there are no attachments into any $u \in S$. All locks incident to $\mathcal{F}(u)$ are now erasible, so by Proposition 20(2) the fuse $\mathcal{F}(u)$ is erasible; by Crucial Property (3) any remaining part of $\mathcal{L}(u)$ follows. Hence all gadgets vanish.

Conclusion. We have produced a sequence of elementary collapses removing all 2-simplices of $Y_r \setminus S'$. Therefore $Y_r \setminus S'$ is erasible. ◀

► **Proposition 23.** *If S is a solution to the ERASIBILITY problem on Y_r , then*

$$S' = \{u \mid Y_r^u \cap S \neq \emptyset\}$$

is a feedback vertex set in D .



■ **Figure 21** A simplicial subcomplex $\cup_{v_i \in C} (\mathcal{F}(Y_r^{v_i}) \cup Cyl_r(v_i, v_{(i \bmod l)+1}))$ of $Y_r \setminus S$ with no free face, leading to a contradiction that S solved erasibility without S' solving FVS.

Proof. We work directly in the final complex Y_r . By the completed construction and the convention that the root bag of the tree decomposition is empty, every vertex lies in F_r . Hence, by the induction hypothesis, each gadget satisfies $\mathcal{L}_B(v) = \mathcal{F}_B(v)$, and all Crucial properties (1)–(5) hold for Y_r .

Assume for contradiction that S makes Y_r erasible but that S' is *not* a feedback vertex set in D . Then $D \setminus S'$ contains a simple directed cycle

$$C = (v_1, v_2, \dots, v_\ell)$$

with arcs (v_i, v_{i+1}) for $i = 1, \dots, \ell$, where indices are taken modulo ℓ . By definition of S' , for each $v_i \in C$ we have $Y_r^{v_i} \cap S = \emptyset$.

Constructing the witness subcomplex. Let

$$Z := \bigcup_{i=1}^{\ell} (\mathcal{L}(v_i) \cup \mathcal{F}(v_i) \cup Cyl(v_i, v_{i+1})) \subseteq Y_r \setminus S.$$

Each cylinder $Cyl(v_i, v_{i+1})$ is, by Crucial Property (5), contained in $\mathcal{F}(v_{i+1})$, and no 2-simplex in Z is deleted by S . Moreover, by the locality of the construction, no 2-simplex outside these gadgets shares an edge with any of the boundary components used in Z . Hence, to test for free 1-simplices in $Y_r \setminus S$, it suffices to inspect Z .

No free edges in Z . In any 2-dimensional simplicial complex, an elementary collapse requires a free 1-simplex—an edge incident to exactly one 2-simplex. We show that no edge of Z satisfies this condition.

(a) *Locks.* By Crucial Property (4), the only potentially free edges of $\mathcal{L}(v_i)$ lie on its boundary $\mathcal{L}_B(v_i)$. At the root, $\mathcal{L}_B(v_i) = \mathcal{F}_B(v_i)$, and by Crucial Property (5) this boundary is glued to the cylinder $Cyl(v_{i-1}, v_i)$. Thus each edge on $\mathcal{L}_B(v_i)$ is incident to one face from $\mathcal{L}(v_i)$ and one from $Cyl(v_{i-1}, v_i)$, both contained in Z . All other edges of $\mathcal{L}(v_i)$ are interior and have two cofaces within $\mathcal{L}(v_i)$.

(b) *Cylinders.* Each $Cyl(v_i, v_{i+1})$ has two boundary circles, attached respectively to a handle in $\mathcal{L}(v_i)$ and to the boundary $\mathcal{F}_B(v_{i+1})$ of the fuse. Hence every boundary edge of a cylinder is incident to one face from the cylinder and one from the corresponding gadget, both in Z . Interior edges of the cylinder have two cofaces within the cylinder.

(c) *Fuses.* The only potentially free edges of $\mathcal{F}(v_i)$ lie on $\mathcal{F}_B(v_i) = \mathcal{L}_B(v_i)$, which is glued to $Cyl(v_{i-1}, v_i)$. Thus each such edge is incident to one face of $\mathcal{F}(v_i)$ and one of $Cyl(v_{i-1}, v_i)$, both present in Z . Interior edges of $\mathcal{F}(v_i)$ have at least two cofaces within the fuse.

Combining (a)–(c), every edge in Z is incident to at least two 2-simplices of Z . Therefore Z contains no free 1-simplex.

Conclusion. Since Z has no free 1-simplices, it cannot be reduced by any sequence of elementary collapses, and is thus non-erasable. But $Z \subseteq Y_r \setminus S$, contradicting the assumption that $Y_r \setminus S$ is erasable. Hence $D \setminus S'$ cannot contain a directed cycle, and S' is a feedback vertex set in D . ◀

C Implementation Details

For reference we include a compact Python implementation of the dynamic program from Section 3. The function `fmo_dp_on_naive_path` implements the four bag types (leaf, introduce-vertex, introduce-edge, forget-vertex) on a “naive” nice path decomposition: we introduce all vertices one by one, introduce all edges in a full bag, and then forget all vertices again. This yields width $|V| - 1$ and is not meant as a practical solver, but as a readable, direct transcription of the state space and transitions.

To validate the implementation, we compared its output with a simple brute-force enumeration of all vertex orders on small instances (typically $|V| \leq 9$), including cases with negative vertex weights. For very small n we additionally enumerated all labelled digraphs and confirmed that the dynamic program and brute force agree on every instance.

■ **Listing 1** Dynamic program for FMO on a naive nice path decomposition

```

def fmo_dp_on_naive_path(instance: FMOInstance):
    """
    Dynamic program for FMO on a naive nice *path* decomposition,
    implementing the DP transitions from the paper for:
    - leaf
    - introduce-vertex
    - introduce-edge
    - forget-vertex

    No join bags appear in this decomposition.
    """
    V = instance.V
    E = instance.E
    w = instance.w

    bags = build_naive_nice_path_decomposition(V, E)

    dp_prev = None # dict[(g_tuple, frozenset(U))] = cost

    for bag in bags:
        btype = bag['type']
        X = bag['X']
        # print("Processing bag:", btype, "X =", X) # uncomment for debugging

        if btype == 'leaf':
            # Unique state: empty order, empty matched set, cost 0
            dp_prev = { (tuple(), frozenset()): 0.0 }

        elif btype == 'introduce_vertex':
            v = bag['v']
            dp_t = {}

```

```

32 # child bag has X without v
33 # from each child state (g, U), we create parent states by inserting v
34 for (g, U), cost in dp_prev.items():
35     g_list = list(g)
36     for i in range(len(g_list) + 1):
37         g0 = tuple(g_list[:i] + [v] + g_list[i:])
38         U_t = U # v is newly introduced and cannot be matched yet
39         key = (g0, U_t)
40         old = dp_t.get(key, inf)
41         if cost < old:
42             dp_t[key] = cost
43     dp_prev = dp_t
44
45 elif btype == 'introduce_edge':
46     u = bag['u']
47     v = bag['v']
48     dp_t = {}
49     for (g, U), cost in dp_prev.items():
50         # Determine relative order of u and v in g
51         pos = {x: i for i, x in enumerate(g)}
52         if u not in pos or v not in pos:
53             # Shouldn't happen in this decomposition
54             continue
55
56         if pos[u] < pos[v]:
57             # Edge is forward -> cannot be in the matching
58             key = (g, U)
59             old = dp_t.get(key, inf)
60             if cost < old:
61                 dp_t[key] = cost
62         else:
63             # Edge is backward and must be in the matching
64             if u in U or v in U:
65                 # Would match a vertex twice -> infeasible, skip
66                 continue
67             U_new = frozenset(set(U) | {u, v})
68             key = (g, U_new)
69             old = dp_t.get(key, inf)
70             if cost < old:
71                 dp_t[key] = cost
72     dp_prev = dp_t
73
74 elif btype == 'forget_vertex':
75     v = bag['v']
76     dp_t = {}
77     wv = w[v]
78     for (g_s, U_s), cost in dp_prev.items():
79         g_list = list(g_s)
80         if v not in g_list:
81             # Shouldn't happen in this decomposition
82             continue
83         idx = g_list.index(v)
84         g_parent = tuple(g_list[:idx] + g_list[idx+1:])
85         if v in U_s:
86             # v already matched -> no extra cost, remove v from U

```

```
        U_parent = frozenset(u for u in U_s if u != v) 87
        new_cost = cost 88
    else: 89
        # v unmatched -> add its weight, U unchanged 90
        U_parent = U_s 91
        new_cost = cost + wv 92
    93
    key = (g_parent, U_parent) 94
    old = dp_t.get(key, inf) 95
    if new_cost < old: 96
        dp_t[key] = new_cost 97
    dp_prev = dp_t 98
    99
    else: 100
        raise ValueError(f"Unknown bag type: {btype}") 101
    102
    # Root bag should be empty; dp_prev has states ((), U) 103
    best = inf 104
    best_state = None 105
    for (g, U), cost in dp_prev.items(): 106
        if cost < best: 107
            best = cost 108
            best_state = (g, U) 109
    110
    return best, best_state 111
```